SYNTHESIS AND CHARACTERISATION OF POROUS POLY (2,5 - BENZIMIDAZOLE) MEMBRANES FOR APPLICATION IN HIGH - TEMPERATURE POLYMER ELECTROLYTE MEMBRANE FUEL CELLS (HT – PEMFCs)

Thesis
Submitted By

ANNESHA DAS

[Class Roll No. 001410302016]
[Examination Roll No. M4CHE1610]
[Registration No. 128889 of 2014 - 15]

Under the Guidance of
PROF. (DR.) KAJARI KARGUPTA

Degree Of Master Of Chemical Engineering.
Department Of Chemical Engineering,
Jadavpur University
Kolkata, India.

DECLARATION

I hereby declare that this thesis contains literature survey and original research work by the undersigned candidate, as a part of her 'MASTER OF CHEMICAL ENGINEERING' studies. All information in this document has been obtained experimentally in accordance with the academic rules and moral conduct.

NAME	ANNESHA DAS
CLASS ROLL NO.	001410302016
RESISTRATION NO.	128889 of 2014-15
EXAMINATION ROLL NO.	M4CHE1610
THESIS TITLE	SYNTHESIS AND CHARACTERISATION OF POROUS POLY(2,5-BENZIMIDAZOLE) MEMBRANES FOR APPLICATION IN HIGH - TEMPERATURE POLYMER ELECTROLYTE MEMBRANE FUEL CELLS (HT – PEMFC)

CERTIFICATE

This is to certify that **MS. ANNESHA DAS,** final year student of Master of Chemical Engineering (M.E. Che) in Department of Chemical Engineering, Jadavpur University bearing a class roll no. 001410302016, Regd. No. 128889 of 2014-15, has completed the project work entitled **"Synthesis and Characterization of Porous Poly(2,5-benzimidazole) membranes for application in High-Temperature Polymer Electrolyte Membrane Fuel Cell"** under the guidance of **PROF. (DR.) KAJARI KARGUPTA** (Professor, Chemical Engineering Department, Jadavpur University) during her Masters curriculum. This work has not been reported earlier anywhere and can be approved for submission in partial fulfillment of the course work.

31/5/16

Prof. (Dr.) Chandan Guha
Head of the Department
Chemical Engineering Department
Jadavpur University.
Kolkata-32

Dr. Chandan Guha
Professor & Head
Chemical Engineering Dept.
Jadavpur University, Kolkata

Kajari Kargupta 30/05/2016

Prof. (Dr.) Kajari Kargupta
Project Supervisor, Professor,
Chemical Engineering Department
Jadavpur University.
Kolkata-32

Professor
CHEMICAL ENGINEERING DEPARTMENT
JADAVPUR UNIVERSITY
Kolkata-700 032

DEAN OF ENGINEERING FACULTY
Jadavpur University,
Kolkata-32

ACKNOWLEDGEMENT

I am grateful to **Jadavpur University, Kolkata** for providing an opportunity to undertake this work. I have been able to gather valuable insight into the intricacies of the process of research work

While doing this project, I have come across many erudite personalities who had helped me a lot in doing and finishing this project simultaneously. It is their kind help and untiring effort that has resulted in completion of this project.

I am deeply indebted to my Project Coordinator **Prof. (Dr.) Kajari Kargupta**, who has rendered her kind help by giving valuable advice and guidance from the very early stage of this research and for encouraging me in every step of work on this project

I am very grateful to **Prof. Chandan Guha**, Head of the Department, Chemical Engineering Department and all other faculty members for their help and cooperation.

I want to thank all the teachers and staff of the Chemical Engineering Department. I am also indebted to **Jadavpur University, Dept. of Chemical Engineering** for support and giving me the opportunity to use the equipments to do my research.

I would like to extend my thanks to our Lab assistant who has helped me a lot all throughout my work. My sincere appreciation also extends to all my colleagues and others who have provided assistance at various occasions; it is not possible to list all of them in this limited space.

I am grateful to my parents who encouraged and supported me all through and helped me in all respect.

Annesha Das. 30/5/16.

ANNESHA DAS

Jadavpur University,
Kolkata, India

ABSTRACT

High Temperature (HT) Polymer Electrolyte Membrane (PEM) Fuel Cells (FC) that work at temperatures of 150-200°C have found applications in combating fossil fuel consumptions in the recent decades due to their high theoretical efficiencies. Commercially available Polybenzimidazole (PBI) membranes doped with phosphoric acid have been a major candidate for role of the solid polymer electrolytic membrane for HT-PEMFCs applications. Poly(2,5-benzimidazole) (AB-PBI) polymer is a cheaper and easily synthesizable variant of PBI that can be prepared from a single monomer. It exhibits a higher capacity to retain dopant acid per imidazolium ring as compared to PBI and consequently, has better proton conductivity at working temperatures.

Present work involves amplifying proton conductivity of ABPBI membranes by modifying them into porous ABPBI (pABPBI) membranes. The first instance of using Sodium Chloride as porogen to prepare porous ABPBI membranes via a solvent evaporation/salt leaching process is reported. The pre-synthesized ABPBI polymer is cast into porous membranes by evaporating a poly(2,5-benzimidazole)/porogen/methanesulfonic-acid (MSA) solution. The porogen is then leached out by repeated washing with water (non-solvent for polymer) until complete removal. The ABPBI and pABPBI membranes are characterised using SEM, FT-IR, NIS d – Elements D, TGA and EIS techniques. SEM images reveal the spherical mesopores and some scattered micropores on the surface of the pABPBI membrane. FT-IR spectroscopy studies of both ABPBI and pABPBI membranes indicate that the introduction of the salt resulted in no significant structural change in the polymer backbone. Water and acid uptake capacities of the pABPBI membrane were enhanced as compared to the ABPBI membrane, and the former reported a maximum proton conductivity of A maximum conductivity of 0.02783 S/cm was achieved for the pABPBI membrane as compared to 0.01019S/cm for ABPBI membrane at 185°C. TGA studies revealed excellent thermal stability of the porous membrane. Thus, the pABPBI membrane demonstrated enhanced acid uptake and proton conductivity when compared with that of the original ABPBI membrane while retaining its structural integrity, suggesting the successful synthesis of a promising new polymer electrolyte for applications in High-Temperture PEMFCs.

Keywords: High- Temperature PEMFC, Polybenzimidazole, ABPBI, porous, proton conductivity, fuel-cell.

CONTENTS

Chapter – I : Introduction: Polymer Electrolytic Membrane Fuel Cells

LIST OF FIGURES

LIST OF TABLES

Chapter - I

Introduction: Polymer Electrolytic Membrane Fuel Cells

1. **INTRODUCTION**
    - **1.1. Components of a Polymer Electrolytic Fuel Cells**
    - **1.2. Electrochemical reactions in a Fuel Cell**
    - **1.3. Energy Efficiency of a Fuel Cell**
    - **1.4. Performance of a Fuel Cell**
    - **1.5. Operating conditions of a Fuel Cell**
    - **1.6. Challenges of a Low - Temperature PEMFC**

-

2. **HIGH TEMPERATURE POLYMER ELECTROLYTIC MEMBRANE FUEL CELLS**
    - **2.1. Benefits of a HT-PEMFC**
    - **2.2. Challenges of a HT-PEMFC**

1. INTRODUCTION

Polymer Electrolytic Membrane Fuel Cells (PEMFC) are a class of environmentally benign electrochemical devices that convert chemical energy stored within the fuel into to usable form of electrical energy, giving a high power density and energy efficiencies of upto 80% on using co-generation models[1]. There are various types of PEMFCs depending upon the choice of fuel viz. direct hydrogen fuel cell, direct methanol fuel cell, direct ethanol fuel cell, and direct formic acid fuel cell.

The major applications of the PEMFCs involve transportation and distributed or stationary and portable power generation units[2-5]. Motor companies prefer working with PEM fuel cells since they exhibit high dynamic stabilities and power densities. [2-3]

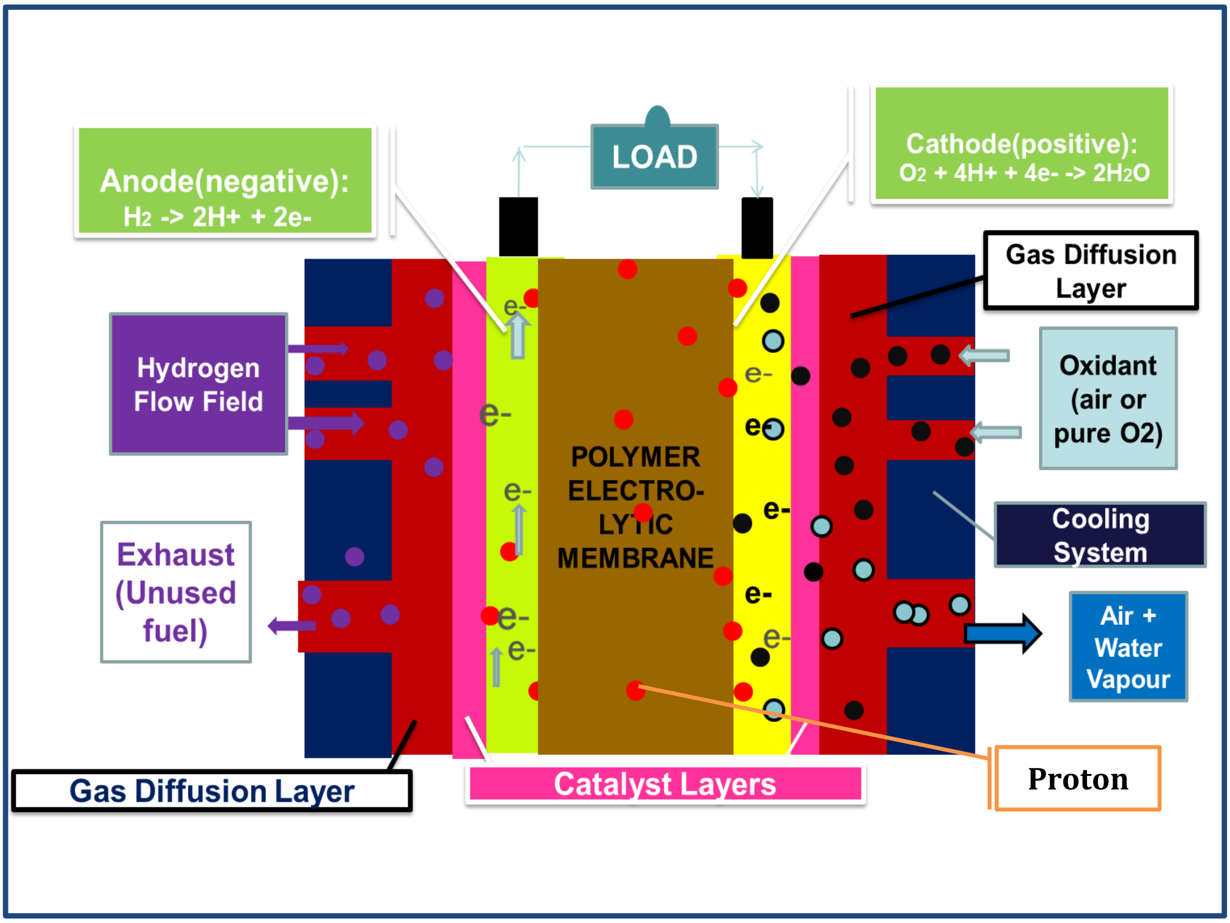

Fig 1.1 . Schematic of the working of a typical PEMFC

For a typical PEMFC set up (Fig 1.1), the anode and cathode of the cell is separated as shown by a polymer membrane that acts as a solid electrolyte. Under working conditions, the fuel (say, H_2) reaches the anode where it is catalytically split at the anode catalyst layer into protons and electrons. These protons are conducted via the membrane to the cathode side, while the electrons are selectively blocked. The electrons are made to travel via an external circuit towards the cathode, giving usable work in the process. Both protons and electrons having reached the anode, react with the oxidant (say, pure O_2), producing heat and water as byproducts. Thus, the entire process gives electricity, water and heat without any harmful byproducts. This makes the fuel cell and its components a focus of vast research in this day and age of energy crisis.

For a H_2/air fuel cell operated at 80°C, the measured OCV is much lower than the theoretical (~1.0 V)[6]. During operation, a single fuel cell generates a cell voltage of around 0.6–0.8 V, depending on the controlled current density, and the MEA has a power density less than 1.0 W/cm^2[6]. Therefore, a single fuel cell is insufficient to supply suitable power for application units and a series of several cells forming a stack is necessary to achieve higher voltage and power density.

Fig 1.2. A single cell of a PEMFC

1.1. Components of a Polymer Electrolytic Fuel Cells

The main components of a PEMFC are :

- i. The Membrane-Electrode Assembly (MEA)
    - a. catalyst coated electrodes
    - b. solid polymer electrolytic membrane
- ii. Grooves for gas flow.
- iii. Current Collectors.

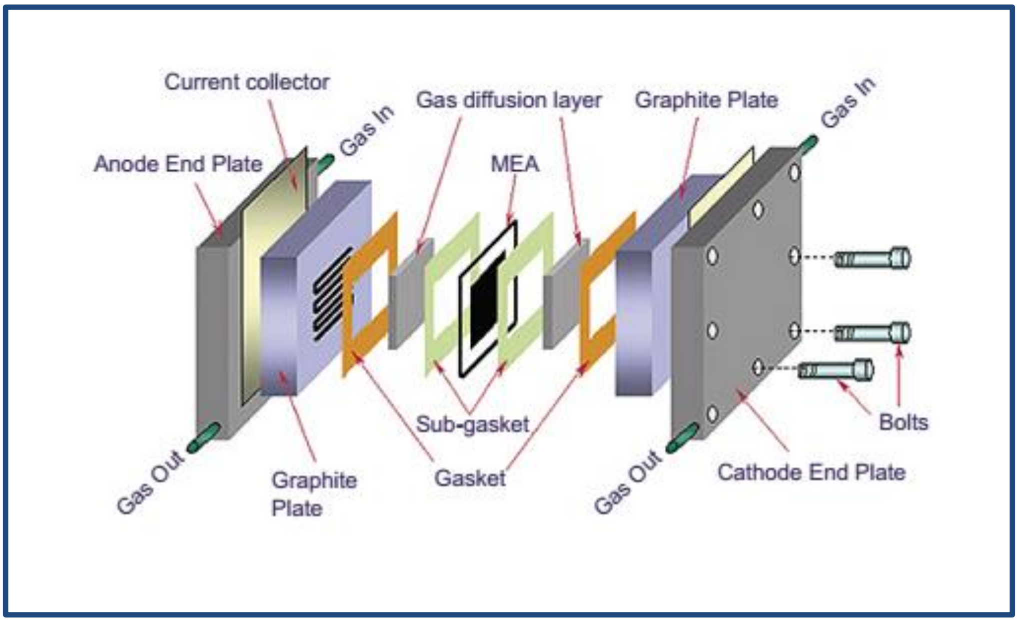

Fig. 1.3. Components of a single cell [6]

❖ Catalysts:

The hydrogen splitting at the anode and combination of the proton, electron and oxygen at the anode occurs catalytically on the electrocatalyst layers. The catalysts layers (CL) usually consist of the catalyst, a proton conducting ionomer and PTFE (polytetrafluoroethylene)[6]. Pt-based catalysts have been the most extensively used catalysts for the purpose, despite their cost [7-16]. The catalyst nanoparticles are usually dispersed over a carbon support (carbon blacks, carbon nanotubes or carbon nanofibers). However, Carbon corrosion at high temperatures may lead to the isolation of the catalysts and thus, deactivation of the catalysts layers[6]. The anode catalyst layer is susceptible to carbon poisoning; thus, CO-tolerant catalysts have attracted attention, including carbon-supported bietallic catalysts like Pt-Ru catalysts [17-19], Pt-Sn catalysts [17,20-21]], Pt-Mo catalysts [22-25], Pt-Au [25-27] catalysts, etc.

❖ Gas diffusion layers

GDLs on either side of the membrane provide support for the catalyst as well as electrical connection between the electrodes and the flow field grooves[6]. They are made porous and hydrophobic, and thus allow the reactant gasses to permeate to the membrane while drawing out moisture[2,28-29].

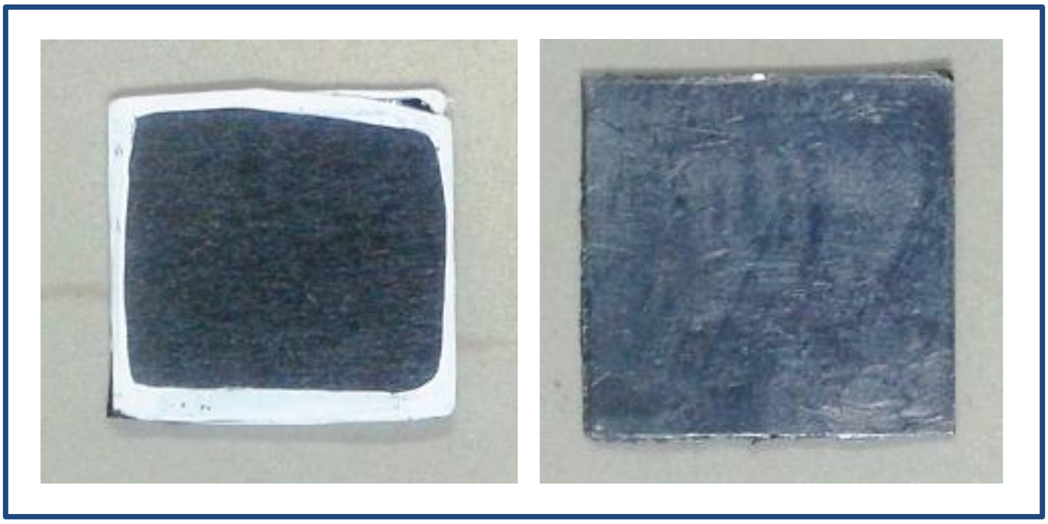

Fig 1.4. (left) Membrane-Electrode Assembly; (right) Graphite gasket

❖ Polymer Electrolytic Membrane:

The polymer electrolytic membrane acts a solid semi-permeable barrier to the transport of protons, forcing of electrons to move through the external circuit. Good membrane properties desired are thus high proton conductivity and thermo-oxidative stabilities while simultaneously having low electron and fuel crossovers[2]. There are several kinds of membranes based on the type of PEMFC. Nafion is a polymer membrane that needs to remain hydrated in order to function and thus have found use in Low Temperature PEMFCs. Use of hydrocarbon based membranes is more preferred in case of high-temperature based PEMFCs[30-31].

❖ Flow field Plates:

Flow field plates are blocks with channels inside of them, where gasses enter from one end of the channel and exit from the other while being in intimate contact with the GDL during their passage through the grooves. For a single cell, flow field plates consist of a block of electrically conductive metal or non-metal with flow channels on one side. The plates give structural support to the MEA as well as provide a connection to the current collector. In case of a fuel cell stack, there are grooves on either sides of this plate and hence, they are called bipolar plates. The intermediate grooves provide connections between two adjacent cells, while end plates connect to the current collector. In either case, flow field plates are required to be chemically and thermally stable, with high electronic conductivities and low gas permeabilities. They are also required to be sturdy, cheap and light. Most commonly used gas flow plates are graphite plates with high electronic conductivity and chemical stability. The design of the grooves affects the distribution of incoming gasses and the removal of water vapours formed [32-35]. Different types of groove patterns viz. pin-type flow field, straight parallel flow field, serpentine flow field, etc. have been reported. [36-37].

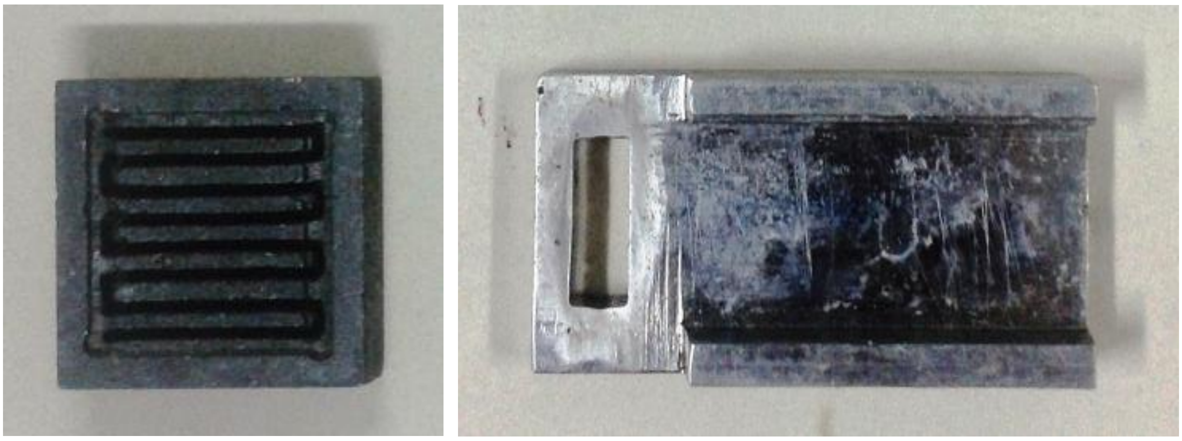

Fig 1.5. (left) Flow field Plate; (right) Current Collector

❖ Current Collectors:

Current collectors placed next to the flow field plates to collect and channelize the current produced within the fuel cell[6]. Electrons produced due to hydrogen splitting at the anode, must travel through the anode to the current collector and then reach the cathode via an eternal circuit. Since the current collectors are usually placed next to the heater, these should possess good thermo-electrical stability and high electron conductivity. Usually, collectors made of copper, stainless steel, titanium, and aluminium are used although non-metallic variants have also been explored[6,38].

- **Additional components:**

Good gaskets with high thermoelectrical and mechanical stabilities are required to safely seal off the connections between the MEA and the flow field grooves. This ensures minimal leakage of gasses out of the cell and direct contact of the reactant gasses is avoided. Sometimes, graphite gaskets are provided between the flow field and the current collector in order to ensure proper passage of electrons. End plates are required to assemble all the components of a fuel cell together.

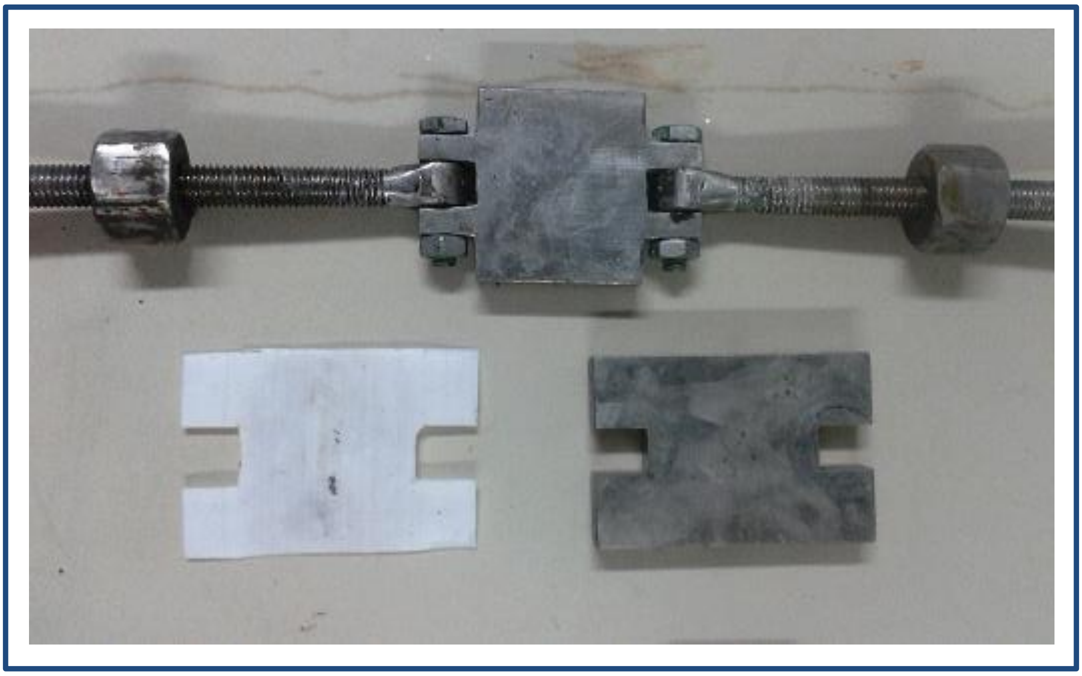

Fig 1.6. Supporting materials of a fuel cell set up.

1.2. Electrochemical Reactions within a Fuel Cell:

In a H_2/O_2 PEMFC, there occurs a series of electrochemical reactions at the catalytic layers of the anode and the cathode, which together converts chemical energy into electrical energy. These reactions maybe given as[6]:

At the anode: $H_2 \longleftrightarrow 2H^+ + 2e^-$ (1.1)

At the Cathode: $O_2 + 4H^+ + 4e^- \longleftrightarrow 2H_2O$ (1.2)

Where, electrochemical reversibility of the reactions is represented by the two direction arrows. At equilibrium for a given temperature, the thermodynamic electrode potentials for reactions 1.1. and 1.2 can then be given by the Nernst equation for each half cell as[6]:

$$E^{r}_{\mathrm{H_2/H^+}} = E^{o}_{\mathrm{H_2/H^+}} + 2.303\frac{RT}{n_{\mathrm{H}}F}\log\left(\frac{a^2_{\mathrm{H^+}}}{a_{\mathrm{H_2}}}\right) \tag{1.3}$$

$$E^{r}_{\mathrm{O_2/H_2O}} = E^{o}_{\mathrm{O_2/H_2O}} + 2.303\frac{RT}{n_{\mathrm{O}}F}\log\left(\frac{a_{\mathrm{O_2}}a^4_{\mathrm{H^+}}}{a^2_{\mathrm{H_2O}}}\right) \tag{1.4}$$

Where,

$E^r_{H2/H+}$ and $E^r_{O2/H2O}$ are the reversible anode and cathode potentials at temperature T, respectively

$E^o_{H2/H+}$ and $E^o_{O2/H2O}$ are the electrode potential of the H_2/H^+ redox couple and O2/H2O redox couple at STP respectively

n_H and n_O are the electron transfer numbers (n_H=2 for the H_2/H^+ redox couple and n_O = 4 for the O_2/H_2O redox couple);

R is the universal gas constant (8.314 J K1 mol1);

and F is Faraday's constant (96,487 C mol1).

Combining Eqn (1.3) and (1.4) the theoretical fuel cell voltage $\mathbf{V_{OCV}}$ (Open Circuit Voltage) can be written as:

$$V^{\mathrm{OCV}}_{\mathrm{cell}} = E^{r}_{\mathrm{O_2/H_2O}} - E^{r}_{\mathrm{H_2/H^+}} \tag{1.5}$$

This value is of V_{cell} is equal to 1.229V, which is the theoretical maximum voltage obtainable from a fuel cell. However, the true value of Open Circuit Voltage obtained in a fuel cell is usually less than 1V, due to factors like mixed potentials and fuel crossovers[39].

1.3. Energy Efficiency of a Fuel Cell:

The collective energy generated during the combustion of hydrogen and oxygen within a fuel cell can be categorised as:

1. Electrical work done against external load
2. Heat released due to fuel cell reaction.

The cumulative energy produced is the same as the heat of formation of water at same temperature and pressure. Considering an infinitely slow fuel cell reaction, these two forms of energy can be written in terms of the overall heat of the reaction as:

$$\Delta H = \Delta G_{cell} - T\Delta S \qquad (1.6)$$

Where,

ΔH is the total heat energy of the overall fuel cell reaction (change in reaction enthalpy),

ΔG_{cell} is the maximum electrical work that can be generated;

$T\Delta S$ is the maximum heat that the fuel cell can release.

The heat output ($T\Delta S$) can only be efficiently harnessed using elaborate co-generation techniques. Also, this additional heat needs to be removed from the system to avoid damage to the fuel cell, even if it cannot be recycled later on. Thus, $\Delta Gcell$ is evidently the desired form of energy output.

The theoretical energy efficiency of a fuel cell (η_{FC}) can then be given as[6]:

$$\eta_{FC} = \frac{\Delta Gcell}{\Delta H} * 100\% \qquad (1.7)$$

Thus, at standard temperature and pressure of 25°C and 1 atm, the theoretical efficiency of a fuel cell is approximately 83%, a value significantly higher than that predicted for the Carnot Engine. However, with an increase in temperature, the η_{FC} will expectedly decrease as the fraction of unusable energy in the form of heat increases. It has been reported that there is a decrease of about 0.0174%/°C in the η_{FC} in the temperature range of 25 °C to 1000°C [40].

The practical values of energy efficiencies differ from this theoretical maximum depending upon the factors like hydrogen utilisation rates and catalysts activities.

1.4. Performance of a Fuel Cell:

The performance of a fuel cell is measured as the power density (mW/cm^2) obtained from the voltage generated and the current density. A typical polarization curve is shown in fig 1.7.

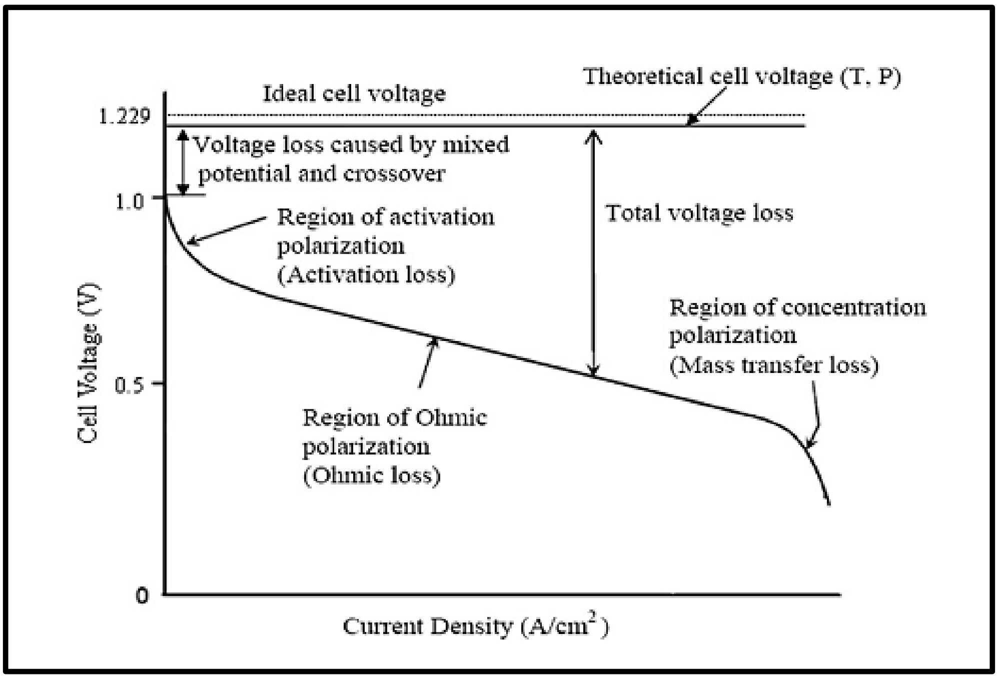

Fig 1.7. Polarization curve for PEMFC [37]

The four regions of losses can be attributed to[37]:

(1) Losses in OCV as a result of H_2 crossover and cathode mixed potential,
(2) Losses incurred due to slow reaction kinetics,
(3) Losses sustained due to membrane resistance, and
(4) Losses due to mass transfer limitation.

1.5. Operating Conditions for a Fuel Cell

1.5.1. Operating Temperature

Fuel Cells that work with membranes like Nafion have operating temperatures below 100°C. This is because the proton conductivity of the membrane is strongly dependant on its moisture content. At temperatures above 90°C, the polymer begins to lose moisture, leading to a sharp drop in fuel cell performances. These type of PEMFCs are called Low Temperature - PEMFC. High Temperature – PEMFCs that work at temperatures ranging from 90-200°C have gained popularity due the factors like improved CO poisoning tolerance, enhanced electrode kinetics and simplified water and thermal managements [1,-2]. Hence, polymeric membranes that can withstand such temperatures while giving adequate proton conductivity are highly desirable. One such class of membranes are the Polybenzimidazole membranes that have been explored extensively. Even though certain advantages are there, the HT-PEMFCs have some drawbacks like decreased Open Circuit Voltage and enhanced degradation of the fuel cell components that need to be addressed.

1.5.2. Operating Pressures within the Fuel Cell

PEMFCs can work under pressures of upto 5 atms. Increased operating pressures result in improved electrode kinetics and better mass transport processes as well as increasing the open circuit voltage, thereby improving fuel cell performances [41]. However, under high working pressures, more power is required to force gasses into the cell, incurring more costs. The usual fuel cell works under pressures of 1-3 atm.

1.5.3. Relative humidity within the Fuel Cell

Relative humidity is defined as the ratio of the amount of moisture present in air at a given temperature to that required to saturate the same air at same temperature. In terms of partial pressures, this may be written as:

$$RH=[p_w(T)/p_{wsat}]*100\% \qquad (1.8)$$

where p_{wsat} is the saturated water vapor pressure at temperature T [6].

For low temperature PEMFCs using membranes like Nafion, the moisture content present in the polymer is of great significance. In order to improve fuel cell performances, it then becomes important to maintain constant humidification within the cell. To achieve this, reactant gases maybe passed through humidifiers before being introduced into the cell. However, increased relative humidity can also cause difficulties in water management inside the fuel cell, which may cause the electrode to "flood". Use of High-Temperature PEMFCs that operate at temperatures between 100-200^{o}C with membranes that can function without or with negligible moisture, are thus favoured to circumvent this problem.

1.6. Challenges of Low - Temperature PEMFCS:

Low temperature PEMFCs refer to those Polymer Electrolytic Fuel Cells that function under 100^{o}C. These usually use membranes like Nafion which need a high degree of hydration in order to function properly. However, at such operating temperatures, there are certain challenges involved[2]. These include:

- ✓ Slow reaction kinetics.
- ✓ Low (<10ppm) carbon monoxide tolerance of platinum and platinum based catalysts and consequent catalyst poisoning.
- ✓ Maintenance of moisture within the PEM to ensure conductivity properties of the membrane.
- ✓ Removal of excess water from the cathode to prevent "flooding".

2. HIGH - TEMPERATURE POLYMER ELECTROLYTIC MEMBRANE FUEL CELLS (HT - PEMFCs):

High-temperature Proton Electrolytic Membrane Fuel Cells (HT-PEMFCs), usually operate at temperatures from 90 to 200^{o}C. The development of HT-PEM fuel cells has been reviewed extensively; vast research has been conducted to mitigate some of the problems associated with so called Low-Temperature PEM fuel cells (LT-PEMFCs) that usually operate below 90^{o}C[1-2,6].

2.1 Benefits Of HT - PEMFCs:

The use of High Temperature PEMFCs help counter some of the problems associated with low-temperature PEMFCs in the following manner:

2.1.1. Enhancement of Electrode Reaction Rate Kinetics:

Exchange current densities for both the hydrogen oxidation reaction at the anode and the oxygen reduction reaction at the cathode are dependent on temperature as

$$i^{o} = i^{o} \exp\left(- E_a/RT\right) \tag{1.9}$$

where,

i^{o} is the exchange current density at the respective electrode at temperature T
i^{o} is the exchange current density at infinitely high temperature
E_a is the activation energy of the particular reaction at respective electrode
R is the universal gas constant.

Thus, an increase in fuel cell temperature favourably increases the exchange current density, thereby improving electrode kinetics.

2.1.2. Higher tolerance towards contaminants:

Incoming fuel streams usually contain various contaminants, the most significant of which is Carbon Monoxide that poisons the Pt based catalyst, effectively deactivating the anode. To counter this, alternative CO-tolerant catalyst preparation [17-27] has been reported, as well as processing incoming fuel [42-43]. However, CO contents as low as 10 ppm may still cause significant damage in LT-PEMFCs. To purify input hydrogen streams to CO contents of less than 10 ppm is a highly cost effective phenomenon. However, increasing the temperature of the PEMFC has been reported to significantly reduce CO poisoning. This is because the CO favourably adsorbs on the catalyst active sites compared to hydrogen, and thus reduces anodic catalyst activity[6,44]. However, since the CO adsorption on catalyst active sites is a phenomenon associated with high negative entropy[45-46], the rise in fuel cell temperatures causes a significant reduction in CO adsorption. Thus, hydrogen fuel streams directly coming from reformers maybe used at temperatures higher than 150^{o}C [6].

2.1.3. Simplified Management of Water:

Water management is a critical issue in PEMFCs. PFSA-based membranes need to be highly hydrated in order to conduct protons efficiently. This demands that inlet gasses be humidified separately before introduction into the cell. Excess moisture at the cathode, where water vapour is already produced as by product, leads to “flooding” of the electrode, causing blockage in the GDL layers and flow fields.

Use of Polybenzimidazole based membranes that use acid dopants (like phosphoric acid) to aid the process of proton hopping are suitable alternatives for HT-PEMFC applications[2]. These do not require additional humidification, and thus, mitigates additional costs of a humidifier system, as well as simplifying the overall system design. Also, mass transfer resistances through the GDL and flow fields are significantly reduced in the absence of moisture and the system may be operated at temperatures as high as 200^{o}C without significant pressure contributions. Chances of residual liquid within the cell components are reduced, thereby leading to lesser degrees of cell degradation when exposed to sub-zero temperatures.

2.1.4. Improved Heat Management:

The use of high temperature fuel cells produces high temperature cooling water, which may be used effectively for other purposes. Rate of heat dispersal is also much faster, reducing required size of the cooling system. Possible integration of the high temperature fuel cell system with a methanol reformer unit is expected to reduce problems of hydrogen storage as well as improve overall efficiency of the plant.

2.2. Challenges Of HT – PEM Fuel Cells

Although operation of PEM fuel cells at high temperatures has many attractive benefits, various cell components experience severe challenges, the most significant problems being loss of moisture from membrane and subsequent decreased conductivity. In addition, Pt particle agglomeration, carbon support corrosion, and degradation of other components such as gaskets, seals, and bipolar plates are accelerated at high temperatures.

2.2.1. Membrane Stability:

The mechanical and thermo-oxidative stabilities of the membranes at high temperatures are points of concern. In an effort to increase proton conductivities, thin membranes are preferred for operation. This increases the risk of gas permeation and mechanical degradation of the membrane under working conditions[6]. Apart from safety concerns, this fuel crossover may also result in higher rate of formation of $HOO^{\bullet}$ and $HO^{\bullet}$ radicals that attack the polymer matrix. This chemical degradation expectedly rises with temperature as reaction rates increase. Thus membrane stability is a major focus of research[47].

2.2.2. Degradation of other components:

Degradation of platinum based catalysts due to Pt agglomeration and particle growth reduces the catalyst activity during long term operation [2]. Carbon oxidation at elevated temperature in the presence of Pt in enhanced[48]. Sealing materials with thermal stabilities above 200°C (eg. silicon rubber, tetrafluoroethylene-propylene, perfluoroelastomer,)[49] should be used.

REFERENCE

1. Papageorgopoulos D. DOE fuel cell technology program overview and introduction to the 2010 fuel cell pre-solicitation workshop in DOE fuel cell pre-solicitation workshop. Department of Energy, Lakewood, Colorado; 2010.
2. Wang Y., Chen K., Mishler J., Cho S.C., Adroher X.C. A review of polymer electrolyte membrane fuel cells: Technology, applications, and needs on fundamental research. Applied Energy 88 (2011) 981–1007.
3. Gittleman C, DM, Jorgensen S, Waldecker J, Hirano S, Mehall M. Automotive fuel cell R&D needs. In: DOE fuel cell pre-solicitation workshop. Department of Energy, Lakewood, Colorado; 2010.
4. Garche J, Jorissen L. PEMFC fuel cell. In: Vielstich W, Gasteiger H, Lamm A, editors. Handbook of fuel cells: fundamentals, technology andapplications. John Wiley & Sons, Ltd.; 2003.
5. Geiger S, Copper MAJ. Fuel cell small stationary market survey. Fuel Cell Today 2003.
6. Jianlu Zhang Huamin Zhang Jinfeng Wu Jiujun Zhang. PEM Fuel Cell Testing and Diagnosis. Copyright (2013) Elsevier B.V.
7. Yu P, Pemberton M, Plasse P. PtCo/C cathode catalyst for improved durability in PEMFCs. J Power Sources 2005;144(1):11–20.
8. Reiner A et al. Co-sputtering: a novel platinum–carbon catalyst preparation method. In: 3rd European PEFC forum, Lucerne; 2005. Poster 109.
9. Ismagilov ZR et al. Development of active catalysts for low Pt loading cathodes of PEMFC by surface tailoring of nanocarbon materials. Catal Today 2005;102–103:58–66.
10. Fernandez JL, Walsh DA, Bard AJ. Thermodynamic guidelines for the design of bimetallic catalysts for oxygen electroreduction and rapid screening by scanning electrochemical microscopy. M–Co (M: Pd, Ag, Au). J Am Chem Soc 2004;127(1):357–65.
11. González-Huerta RG, Chávez-Carvayar JA, Solorza-Feria O. Electrocatalysis of oxygen reduction on carbon supported Ru-based catalysts in a polymer electrolyte fuel cell. J Power Sources 2006;153(1):11–7.
12. Rao CRK, Trivedi DC. Chemical and electrochemical depositions of platinum group metals and their applications. Coord Chem Rev 2005;249(5–6):613–31.
13. Pharkya P, Alfantazi A, Farhat Z. Fabrication using high-energy ball-milling technique and characterization of Pt–Co electrocatalysts for oxygen

reduction in polymer electrolyte fuel cells. J Fuel Cell Sci Technology 2005;2:171–7.

14. Travitsky N et al. Nanometric platinum and platinum-alloy-supported catalysts for oxygen reduction in PEM fuel cells. In: 3rd European PEFC forum, Lucerne, Switzerland; 2005.
15. Wells P et al., Preparation of Cr/Pt/C catalysts by the controlled surface modification of Pt/C using an organometallic precursor. In: 3rd European PEFC forum, Lucerne, Switzerland; 2005.
16. Xie J et al. J Electrochem Soc 2005;152(1):A104–13
17. Lee D, Hwang S, Lee I. J Power Sources 2005;145:147–53.
18. Ioroi T, Akita T, Yamazaki S-i, Siroma Z, Fujiwara N, Yasuda K. Electrochim Acta 2006;52: 491–8.
19. Pitois A, Pilenga A, Tsotridis G. Appl Catal A 2010;374:95–102.
20. Lim D-H, Choi D-H, Lee W-D, Lee H-I. Appl Catal B 2009;89:484–93.
21. Lee SJ, Mukerjee S, Ticianelli EA, McBreen J. Electrochim Acta 1999;44:3283–93.
22. Santiago EI, Camara GA, Ticianelli EA. Electrochim Acta 2003;48:3527–34. [46] Papageorgopoulos DC, Keijzer M, de Bruijn FA. Electrochim Acta 2002;48:197–204.
23. Ordo ́n ̃ez LC, Roquero P, Sebastian PJ, Ramı ́rez J. Int J Hydrogen Energy 2007;32:3147–53.
24. Lebedeva NP, Janssen GJM. Electrochim Acta 2005;51:29–40.
25. Ma L, Zhang H, Liang Y, Xu D, Ye W, Zhang J, et al. Catal Commun 2007;8:921–5.
26. Wang J, Yin G, Liu H, Li R, Flemming RL, Sun X. J Power Sources 2009;194:668–73.
27. Herna ́ndez-Ferna ́ndez P, Rojas S, Oco ́n P, de Frutos A, Figueroa JM, Terreros P, et al. J Power Sources 2008;177:9–16.
28. Mathias M et al. Handbook of fuel cells: fundamentals. In: Vielstich W, Gasteiger H, Lamm A, editors. Technology and applications. John Wiley & Sons, Ltd.; 2003.
29. Larminie J, Dicks A. Fuel cell systems explained. John Wiley & Sons; 2000.
30. Ma Y-L et al. Conductivity of PBI membranes for high-temperature polymer electrolyte fuel cells. J Electrochem Soc 2004;151(1):A8–A16.
31. Zhang J et al. High temperature PEM fuel cells. J Power Sources 2006;160(2):872–91.
32. Kumar A, Reddy RG. J Power Sources 2003;113:11–8.
33. Kumar A, Reddy RG. J Power Sources 2006;155:264–71.

34. Yoon Y-G, Lee W-Y, Park G-G, Yang T-H, Kim C-S. Int J Hydrogen Energy 2005;30:1363–6.
35. Yoon Y-G, Lee W-Y, Park G-G, Yang T-H, Kim C-S. Electrochim Acta 2004;50:709–12.
36. Li X, Sabir I. Int J Hydrogen Energy 2005;30:359–71
37. Zhang J, Zhang J. In: Zhang J, editor. PEM fuel cell electrocatalysts and catalyst layers fundamentals and applications. London: Springer; 2008. p. 965–1002.
38. Hentall PL, Lakeman JB, Mepsted GO, Adcock PL, Moore JM. J Power Sources 1999;80: 235–41.
39. Zhang J, Tang Y, Song C, Zhang J, Wang H. J Power Sources 2006;163:532–7.
40. Larminie J, Dicks A, editors. Fuel cell systems explained. John Wiley & Sons, Ltd; 2003.
41. Zhang J, Li H, Zhang J. ECS Trans 2009;19:65–76.
42. Gottesfeld S, Pafford J. J Electrochem Soc 1988;135:2651–2.
43. Schmidt V, Oetjen H, Divisek J. J Electrochem Soc 1997;144:L237–8
44. Zhang J, Xie Z, Zhang J, Tang Y, Song C, Navessin T, et al. J Power Sources 2006;160: 872–91.
45. Dhar H, Christner L, Kush A. J Electrochem Soc 1987;134:3021–6.
46. Vogel W, Lundquist L, Ross P, Stonehart P. Electrochim Acta 1975;20:79–93.
47. Wei Qian, Yuming Shang, Shubo Wang, Xiaofeng Xie, Zongqiang Mao. Phosphoric acid doped composite membranes from poly (2,5-benzimidazole) (ABPBI) and CsxH3-xPW12O40/CeO2 for the high temperature PEMFC. Int. J. Hydrogen Energy. 38 (2013) 11053-11059.
48. Kangasniemi KH, Condit DA, Jarvi TD. J Electrochem Soc. 2004;151:E125–32.
49. Parker O-ring handbook, section II, basic O-ring elastomers, P2-11. Cleveland, OH: Parker Hannifin Corporation, http://www.parker.com/o-ring/Literature/ORD5700.pdf; 1999.

Chapter - II

Literature Review: Membranes for High-Temperature PEMFCs

1. INTRODUCTION

The Polymer Electrolytic Membrane (PEM) is a key component of the PEMFC, acting as a selective barrier for proton transfer while forcing electrons to move through an external circuit. The primary requirements for a suitable PEM are thus:

- Ability to conduct protons efficiently within the temperature range of the PEMFC.
- Low fuel crossover/permeability.
- Mechanical, thermal and oxidative stability under working conditions.
- Cheap and environment friendly.

Conventionally used perfluorosulphonic acid based membranes (eg. Nafion®) in HT-PEMFCs are reported to have excellent chemical and mechanical stabilities, along with high proton conductivities. However, they only function in a highly hydrated environment, thereby reporting a sharp decline in fuel cell performances beyond 90oC. Much research has gone into the development of alternative membranes, viz. partially fluorinated membranes, nonfluorinated (including hydrocarbon) membranes, nonfluorinated composite membranes, etc. Amongst them, hydrocarbon based membranes have attracted attention due to their low costs.

1.1. Benefits of using Polybenzimidazole membranes in HT-PEMFC:

After the first proposal to use Polybenzimidazole (PBI) for preparing acid doped membranes [1], significant research has gone into the development and characterisation of the same [2-9] to further understand the advantages provided in the simplified functioning of High Temperature-Polymer Electrolytic Membrane Fuel Cells (HT-PEMFCs). Acid doped PBI membranes and their derivatives are reported to have high proton conductivities [9-14] and thermal stabilities [15] upto 200^{o}C while using several different fuels viz. Hydrogen, Methanol, Alkanes, etc. (reference) These heterocylic polymers, when doped with suitable acids, are found to eliminate the need for hydration as vehicle for proton hopping [16-21]. This has led to the effective design and utilisation of comprehensive HT-PEMFCs with high CO tolerances [22] at low humidification[23] conditions, and better heat utilisation [24-25].

2. POLYBENZIMIDAZOLE MEMBRANES

PBI was first prepared by Vogel and Marvel in 1961 [26] (fig 1). They proposed a heterogeneous, two-step process for PBI formation using tetraaminobiphenyl (TAB) and Diphenyl Isophthalate (DPIP) as monomers [27], which was simplified by Choe at al. [28-29] into a single step process by substituting DPIP with Isophthalic acid (IPA) in the presence of organophosphorus and silicon compounds as catalysts (Fig 2).

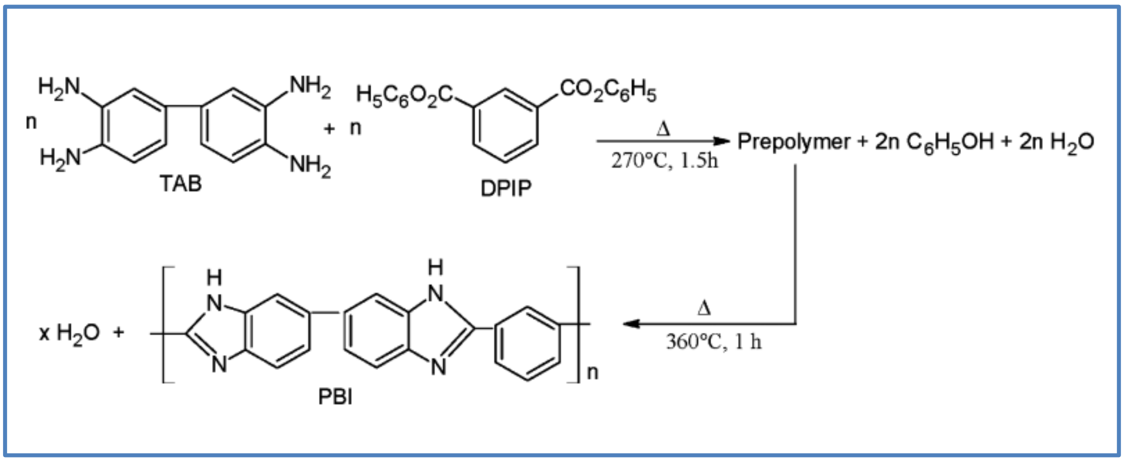

Fig 2.1. Two step method for PBI synthesis as proposed by Vogel [26]

However, the latter still involved temperatures over 300°C. A simpler, homogenous process involving polyphosphoric acid (PPA) as a solvent and a condensation reagent as suggested by Iwakura et al. [30] allowed the polymerisation to occur at much lower temperatures (around 200°C). Xiao et al. [31-32] developed a sol-gel method to directly cast PBI membranes from PBI solutions in PPA, which upon hydrolysis gave PA-doped PBI without further treatment. Eaton’s reagent (synthesized by Eaton et al.) (ref) is an alternative that has found much popularity [33]; it is a mixture of Methanesulfonic acid (MSA) and highly hygroscopic Phosphorous Pentoxide (P_2O_5) thatprovides a less viscous and cheaper alternative to PPA. Trifluroacetic acid (TFA) cast membranes use the polymer powder mixed with TFA and Phosphoric acid whereby the soft, rubbery membranes are prepared by drying the solution cast over a glass plate [34]. Membranes cast using highly polar, aprotic organic solvents such as dimethyl sulphoxide (DMSO), N,N-dimethylforamide (DMF), DMAc, and N-methylpyrrilidone (NMP) require further acid doping in order to achieve suitable proton conductivities.

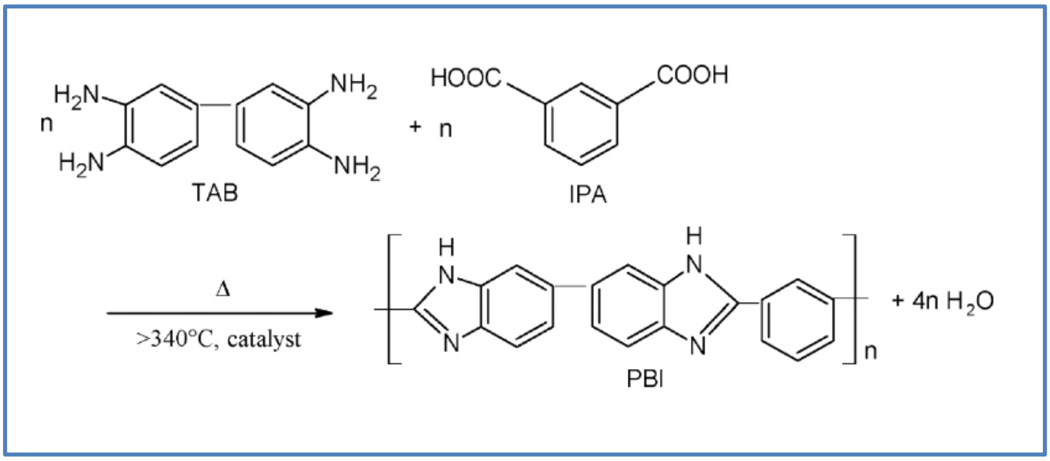

Fig 2.2. Single step method for PBI synthesis as proposed by Choe [28,29]

Vast amount of research has gone into the modification of the primitive polymer in order to enhance properties like solubility, and structural, thermal and chemical stabilities. For membrane casting purposes for fuel cell applications, high molecular weight polymers (with higher degree of polymerisation and crosslinking) are preferred since these correspond to greater mechanical and oxidative stabilities in the acid environment and high temperatures under which the cells work. For proton conductivity enhancements, modifications introduced would primarily consist of hygroscopic fillers (increases moisture retention at lower relative humidity) or conducting composites (reduces water and fuel crossovers).

In general, Polybenzimidazoles refer to a class of aromatic heterocyclic polymers containing the benzimidazole units. Modifications may be introduced by choosing different monomers, or by incorporation of different functional groups at the reactive benzimidazole N–H sites after polymerisation/during membrane casting.

2.1. Variations in Monomers:

Extensive work on modified PBI has been well reviewed [35-36]. Polymers where there has been an incorporation of a pyridine group (by using pyridine dicarboxylic acids) in place of the phenyl ring have reported higher degrees of acid retention and hence proton conductivity. This is expectedly due to the presence of additional N/NH groups in the form of aromatic heterocycles which allows higher basicity while maintaining the intrinsic thermo-oxidative stabilities [32,37-38]. N/NH group incorporation was also carried out in several other different ways by Carollo et al. [37] On the other hand, studies by Schuster et al. [38], Qing et al. [39], and several others indicate that the introduction of ethers and sulphones groups causes a reduction in thermo-chemical stabilities while allowing higher degrees of dissolution and processability. Poly(2,5-polybezimidazole) (ABPBI) was first synthesized using 3,4-diaminobenzoic acid as a monomer in a polyphosphoric acid [26] and later in various other combinations involving methanesulfonic acid, phosphorous-pentoxide and PPA. [ref] The use of a single, easily available monomer simplified the polymerisation process while the addition of an extra N into the repeat unit of the polymer enhanced proton conductivity.

2.2. Variations in Membranes post polymerisation:

An increase in acid doping levels is expected to enhance the proton conductivities. However, this is associated with a simultaneous decrease in the mechanical strength of the membranes. To strike a balance, research has been focussed on the cross-linking of the polymer to enhance mechanical and thermal strengths, along with preparation of membrane composites using various organic and inorganic fillers.

- **Incorporation of Ionic Crosslinkers**
  Kerres et al. [40] reviewed the preparation of flexible ionomer networks from acid–base polymers by ionically cross-linking polymeric acids and polymeric bases. However, ionically cross-linked membranes were reported to exhibit poor thermal stabilities as the cross links disintegrate at higher temperatures in aqueous medium. Also, further doping of these membranes with phosphoric acid led to the formation of ternary membranes with improved mechanical properties but decreased chemical stabilities. Kerres et al. [41-42]

introduced a covalent cross linker into an already ionically cross-linked PBI resulting in a covalent - ionically cross-linked membrane with high conductivity and acceptable swelling and stabilities.

- **Incorporation of Covalent Crosslinkers:**
  The imidazole groups of the polybenzimidazole membrane can be cross-linked using an organic acid or its halide with two or more functional groups per molecule[43]. Though tougher than its non-cross linked adaptation, the covalently cross linked membranes tend to become brittle as they dry out. PBI membranes with Dibromo-p-xylene (DBpX) as the crosslinker exhibited acid-doping level of 8.9 per repeat unit, while possessing comparable mechanical strength to that of linear PBI at an acid- doping level of 6 per repeat unit. Proton conductivity values doubled while chemical stabilities reported no appreciable change. [44]

- **Organic/Inorganic Composite membranes:**
  Apart from enhancing mechanical stabilities and proton conductivity, inorganic fillers can be used to enhance an array of other properties viz. thermal and mechanical stabilities, water and acid retentions, fuel crossovers etc. For example, addition of a hygroscopic moiety (say, silica based composites) to an ionomer would likely result in an increased water retention while increasing stiffness [35]. As reviewed by Li et al.[35], PBI and PBI blend composites inorganic proton conductors (including zirconium phosphate, phosphotungstic acid, silicotungstic acid and boron phosphate) have been reported. PBI/ZRP composite membranes when doped with phosphoric acid reported high conductivities of 9.0×10^{-2} S/cm at 5% RH and 200°C[13]. Introduction of graphene into the Polybenzimidazole matrix results in a marked increase in the mechanical strength.[59]

- **Use of Porogens:**
  Use of various porogens like dimethyl, diethyl, dibutyl, and diphenyl phthalates[48], glucose and sacharose[49]and ionic liquids[50] has been reported for preparing porous PBI membranes with enhanced acid uptake and proton conductivities. Use of crosslinkers [52] alongside porogens has allowed preparation of membranes with good mechanical strengths, that had been otherwise compromised due to the porous matrix.

3. POLY (2,5-BENZIMIDAZOLE) (AB - PBI)

ABPBI synthesis may follow the process shown in Fig. 2.3[26]. However, several other approaches have also been explored as reviewed by Asensio. Wainright et al.[52] reported ABPBI polymers with intrinsic viscosities as high as 7.33 dl/gm by recrystallizing the monomer, to give membranes of extremely high mechanical strength. However, Asenio et al. [54] enumerated that the use of polymers with intrinsic viscosities of 2.3-2.4dl/gm were sufficient to cast membranes of suitable thermal and mechanical strength.

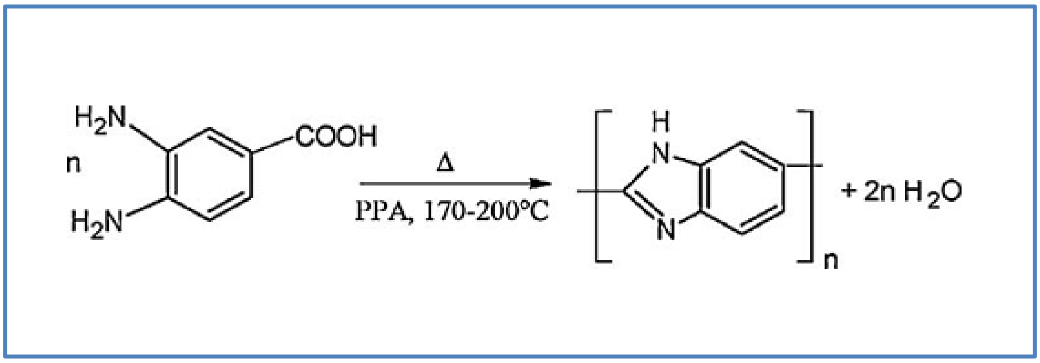

Fig 2.3. ABPBI Preparation Process [26]

3.1. Advantages of ABPBI over PBI:

Asensio et al. [53-54] conducted a comparative study between acid doped PBI and ABPBI to report similar fuel cell performances for both membranes at similar acid-doping levels (power densities of 185mW/cm^2 for PBI membranes and 175mW/cm^2 for ABPBI membranes). The advantages offered by the latter however, were:

- The use of a single, commercially available and environmentally friendly monomer.
- Simpler method of synthesis since only a single monomer is involved.
- Better solubility.

A literature review on the present state of the art of ABPBI polymer and its membranes is tabulated below.

Membrane	Modification	Property Enhancement
ABPBI [54]	Preparation of ABPBI using a poly(2,5-benzimidazole)/phosphoric acid/methanesulfonic acid (MSA) solution.	Simultaneous doping and casting of the membrane was achieved in a simpler way while conductivity properties were somewhat lowered due to evaporation of PA during membrane casting. ABPBI × 3 H_3PO_4 exhibited a conductivity of 1.5×10^{-2} S/cm under dry conditions at 180◦C, good enough for PEMFC application.
ABPBI [55]	Preparation of ABPBI by the polymerization of 3,4-diaminobenzoic acid in a polymerization medium consisting of methanesulfonic acid (MSA) and phosphorous pentoxide.	A maximum conductivity of 0.026S/cm was obtained for the ABPBI x 1.2 H_3PO_4 membrane at 180◦C. A maximum power density of 150mW cm^{-2} was obtained.
ABPBI-PVPA [56]	Blends of ABPBI and Poly(vinylphosphonic acid) were prepared of different stoichiometric ratios.	The protonated and non-protonated N_2 in the ABPBI heterocycle and the PVPA phosphate groups enhanced proton transfer. A highest value of $4X10^{-3}$ S/cm for ABPBI:PVPA (1:4) at 20^{o}C (RH = 50%) was reported.
ABPBI : $Cs_xH_{3-x}PW_{12}O_{40}$/ CeO_2 [57]	$Cs_xH_{3-x}PW_{12}O_{40}$ / CeO_2 nanoparticles were synthesized and used to make composite membranes with ABPBI.	Introduction of the nanoparticles inhibited free radical attacks on the polymer matrix, thereby increasing chemical stabilities. Under humidification, proton conductivities of upto 20mS/cm were reported in the 140-180^{o}C range under humidification.

Membrane	Modification	Property Enhancement
SABPBI [58]	Pristine ABPBI membranes were doped in Sulphuric acid, after which they were heat treated at 450oC for 5 mins exposed to air.	Degree of sulfonation was reported to increase the degree proton conductivities of the membranes. SABPBI membranes with degree of sulfonation of 41% and doped with phosphoric acid (SABPBI x 4. H_3PO_4) reported a maximum conductivity of 3.5 X 10^{-2} S/cm under anhydrous conditions at 180°C.
SPAES/ ABPBI-GO [59]	ABPBI-GO was prepared by reacting DABA with pristine GO. The composite was then incorporated into a Sulfonated poly(arylene ether sulfone) (SPAES) matrix to give SPAES/ABPBI-GO composite membranes	The imidazole unit of the ABPBI and the sulfonic acid unit of the SPAES matrix interacted in an acid-base interaction. This resulted in enhanced mechanical stabilities as and proton conduction due to additional alternative pathways for proton hopping. A conductivity of 152.5 mS/cm was reported for the SPAES/ABPBI-GO (1.0%) membrane at 80°C and 90% RH condition. At higher ABPBI-GO contents, due to ineffective dispersion of the filler, the conductivity values were found to decrease.
ABPBI - $H_3PMo_{12}O_{40}$ [60]	Previously prepared ABPBI polymer and phosphomolybdic acid were simultaneously added to SA and ABPBI-$H_3PMo_{12}O_{40}$ composite membranes were cast.	Under anhydrous conditions, a maximum proton conductivity of 0.003 S/cm was reported for the ABPBI - 45% PMo_{12} composite membrane at 185°C.

Membrane	Modification	Property Enhancement
ABPBI/ POSS [61]	Different POSS particles with core diameters less than 0.6nm were used to prepare ABPBI/POSS.	ABPBI/POSS composite membranes reported enhanced mechanical properties. The hygroscopic, "cage-like" POSS cores contributed towards higher uptakes of acid and water and correspondingly higher proton conductivities higher than 0.1S/cm were reported for ABPBI/OA - POSS X 241% H_3PO_4 membranes in the temperature range of 120-180°C under anhydrous conditions.
ABPBI/CNT [62]	Insitu polymerisation of DABA was carried out with single walled (SW) and multiple walled (MW) Carbon nanotubes (CNT) in phosphoric acid.	Homogenous ABPBI/CNT composite membranes with improved tensile properties (toughness ~ 200MPa) were obtained. Compared to the proton conductivity of pristine ABPBI (4.81×10^{-6} S/cm), ABPBI/SWCNT and ABPBI/MWCNT reported maximum proton conductivities of 9.10 x 10 -5 and 2.53×10^{-1} S/cm respectively.
ABPBI/ mMMT [63]	Organically modified montmorillonite (mMMT)/ABPBI composite were synthesized by mixing variable ratios of polymer and the nano composite in DMAc.	Oxidative degradation of the composite membranes as compared to pristine membranes were reduced with an increase in activation energy of the degradation reaction.

Membrane	Modification	Property Enhancement
ABPBI/SiO_2 [64]	ABPBI - Silica nano composite membrane were prepared exsitu using MSA.	Sulphonated silica particle enhanced thermal stabilities and proton conductivity of the composite membrane as compared to pristine ABPBI. Proton conductivity of 0.380 S/cm was obtained for ABPBI/wt % modified silica at 140˚C, compared to 0.152 S/cm for pristine ABPBI membrane.
ABPBI/IL-SiO_2 [65]	Two types of silica (USB and UMC) with two different pore diameters and sizes were modified using Ionic Liquids. They were then mixed in different ratios with ABPBI in MSA and cast into composite membranes.	Dispersion of Silica in the polymer was improved on modification with the ionic liquids, improving thermo-mechanical properties. A maximum proton conductivity of about 0.067 S/cm was reported for the PA-doped composite membrane comprising 5wt% functionalized UMC (dA5MIL) at 150^{o}C.
(AB-pPBI-X) [66]	Poly{(2,5-Benzimidazole)-co-[2,2’-(p-Phenylene)-5,5’-Bibenzimidazole]} (AB-pPBI-X) polymers were prepared by polymerisation of DABIT with DABA and teraphthalic acid in polyphosphoric acid. X was used to denote the mole % of DABA.	Inherent viscosities of the co-polymers ranged from 4.36-5.76 dl/g which were higher than corresponding homo polymers of ABPBI (4.07dl/g) and pPBI (3.22 dl/g). The solubility and acid uptake properties of the AB-pPBI-X membranes were higher than the homopolymers. Also, AB-pPBI-X demonstrated a tensile strength thrice than that of m-PBI membrane under similar acid doping levels. Proton conductivity of 0.15 S/cm was reported at 180˚C under anhydrous conditions.

Membrane	Modification	Property Enhancement
ABPBI/ PSSA [67]	Blend polymer membranes of ABPBI and poly(styrene sulfonic acid) (PSSA) in different molar ratios were prepared in trifluroacetic acid	Homogeneous polymer blends with enhanced water uptake and proton conductivity were reported. ABPBI PSSA (1:4) membrane reported proton conductivity of 10^{-3} S/cm at elevated temperatures while ABPBI PSSA (1:2) measured proton conductivity of 0.02 S/cm at room temperature. Suitable thermal mechanical stability were also reported.
cABPBI [68]	Cross-linked ABPBI membranes were prepared by reaction of DABA with 1,3,5-Benzene tricarboxylic acid at various mole ratios using 3,3'-diaminobenzenine (DABI)	Membranes exhibited high chemical and mechanical stabilities in phosphoric acid after cross linking the degree of which varied with variations in the mole ratios of DABA, BTCA and DABI. The cABPBI 50 reported a phosphoric acid uptake of more than 84 wt% and a proton conductivity of 0.12 S/cm in dry conditions at 150˚C
ABPBI/(T–PWA–SiO_2) [69]	SiO_2 rivetted phosphotungstic acid (T–PWA–SiO_2) were introduced in various amounts in the polymerisation solution of ABPBI in PPA to prepare ABPBI/(T–PWA–SiO2) composite membranes.	ABPBI/(T–PWA–SiO_2) composite membranes were reported to have enhanced durability and proton conductivity. An approximated conductivity of 5.5×10^{-2} S/cm at 180^{o}C was reported for the ABPBI/(T–PWA–SiO2) (46 wt%) membrane.

Membrane	Modification	Property Enhancement
ABPBI/ PAMPS [70]	Poly (2-acrylamido-2-methyl-1-propanesulfonic acid) (PAMPS)/water solutions were mixed with ABPBI/TFA solutions in variable ratios to cast ABPBI:PAMPS membranes.	Homogeneous polymer blends with heightened water retention and proton conductivity capacities were reported. Thermal stabilities of upto 190°C were observed; thereafter PAMS degraded. ABPBI : PAMPS (1:2) blend membranes exhibited a proton conductivity of 0.1 S/cm under 50% RH.
ABPBI/ SPEEK [71]	Previously prepared SPEEK and ABPBI polymers were mixed in variable ratios and cast using MSA to give blend ABPBI/SPEEK membranes.	ABBPBI/SPEEK membranes 16% Sulfonation Degree – SPEEK was found to exhibited a significant increase in proton conductivity values (a maximum conductivity of 1.09×10^{-1} S/cm at 100°C, compared to a maximum of 1.8×10^{-2} S/cm at 120°C for ABPBI.
ABPBI/ BPO_4 [72]	BPO_4 nanoparticles were preblended with DABA monomer in MSA by dispersion before polycondensation. In another method, BPO_4 nanoparticles were also dispersed in ABPBI solution post-polymerisation. It was observed that pre-blended BPO_4 - ABPBI composite membranes reported better properties than post-blended ones.	Methanol permeability for the composite membranes was reported to decrease to about half of that for pure membranes. PA-doped BPO4-ABPBI membranes exhibited enhanced water and acid uptake capacities, and correspondingly, higher proton conductivities. For pre-blended BPO4-ABPBI membrane with 25% BPO4, a maximum proton conductivity of 0.273 S/cm was observed.

Membrane	Method	Property Enhancement
ABPBI/ CeSPP [73]	Cerium sulfophenyl phosphate (CeSPP) was introduced in various ratios in the polymerisation mixture of DABA in PPA and membranes were cast by hot-pressed method.	Composite membranes were homogenous and exhibited suitable thermal stabilities in the working temperature range of the PEMFC. Highest conductivity of about 14 mS/cm was reported by the ABPBI/CeSPP membrane containing 38% CeSPP at 180°C.
ABPBI/ZPP [74]	Zirconium Hydrogen phosphate and DABA was used to prepared zirconium pyrophosphate/ABPBI composites in polyphosphoric acids.	Addition of 10 - 20% ZPP into the ABPBI led to enhance thermal and mechanical stabilities. A high proton conductivity (0.12 S/cm at 180˚C) was reported.
ABPBI/ZrO_2 [75]	ABPBI/ZrO_2 composite membranes were prepared by incorporating ZrO_2 nanoparticles into ABPBI solution in MSA in different percentages.	A maximum conductivity of 0.069S/cm was reported for composite membrane containing 10% ZrO_2 at 100◦C, more than three times higher than the 0.018 S cm−1 at 120◦C reported for pristine ABPBI. Thermo-mechanical properties were also enhanced.
Porous ABPBI [76]	Porous ABPBI membranes were prepared using surfactants (sodium dodecyl sulphate).	Incorporation of pores resulted in a maximum conductivity of 2.23 X10^{-2} S/cm was achieved for the porous membranes as compared to 1.1 X 10^{-2} S/cm for the pristine ABPBI at 180°C under anhydrous conditions.

4. POROUS POLYBENZIMIDAZOLE MEMBRANES

Porous polymers have found a wide acceptance for multivarious applications including, but not limited to, tissue engineering[77-78], bone grafting[ref], lithium batteries[79] and PEMFCs [76,81-84]. Design and use of an array of organic and inorganic porogens for use as templates to obtain specific structural pores has thus been the focus of vast research. The preparation of such highly porous polymer scaffolds and membranes has been possible using techniques like solvent casting and selective porogen leaching [82-84], gas foaming[85], phase separation [86-87] amongst others [88-91], chosen specifically with the end application in mind. The polymer(s) thus formed exhibit open or closed pores with a size range varying from few micrometers to less than a few nanometers. Based on their sizes, pores are classified as per IUPAC standards as macro-, meso- and microporous depending on the size of the pores > 50 nm, 50–2 nm and <2 nm respectively (Fig 2.)

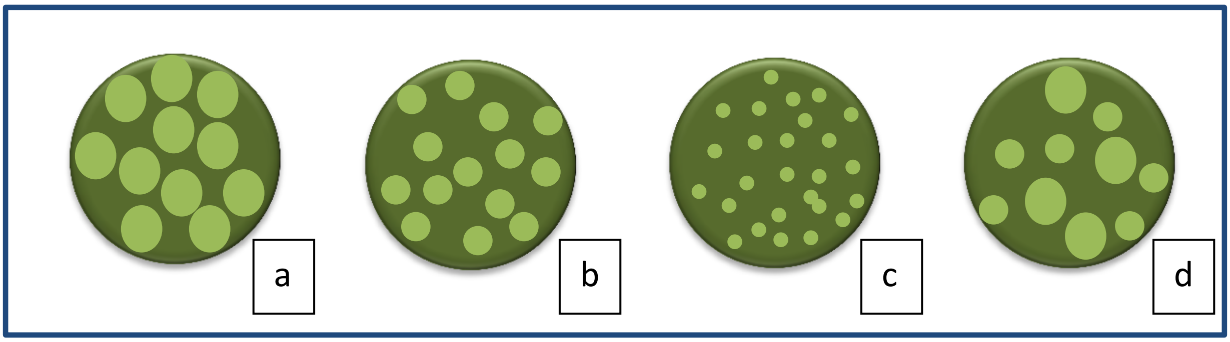

Fig 2.4. Schematic representation of pores based on sizes: (a) unimodal macropores (>50nm); (b) unimodal mesopores (50-2nm); (c) unimodal micropores (<2nm); (d) bimodal pores with more than one type of pore.

The size distribution of pores depends largely on the following factors:

i. Monomer type and ratios of feed to porogens(s).
ii. Nature and combination of porogens used.
iii. Reaction conditions, viz. polymerisation technique, reaction temperature, agitation speed, etc.

Some common types of porogens investigated include organic solvents of variable molecular weight. Examples of low molecular weight solvent porogens include toluene, hexane, cyclohexanone, 2-ethylhexanol, p-xylene, n-heptane [91-

94] and an example of a higher molecular weight solvent is poly(ethylene glycol) [94-95]. On the other hand, inorganic porogens include sodium chloride [96-99], silica [97] and sodium hydrogen carbonate [99].

The incorporation of porosity into the matrix of a polymer electrolyte membrane is expected to increase the dopant uptake percentage, thereby increasing ionic conductivity. While the idea was previously used to prepare porous membranes for lithium battery applications [79-80], pioneering work was done by Zaidi et. al.[81] in preparing porous polyoxadiazoles membranes doped with phosphoric acid for PEMFC application. Thereafter, many groups have reported the preparation of porous PBI membranes using different porogens[48-49,]. Mecerreyes et. el. [48] used different phthalates and phosphates for porous PBI membrane preparation, reporting that shape and size of the pores became larger and more erratic with increasing porogen/polymer ratios and porogen molecular weight. Highly porous films with enhanced acid uptake capacities were synthesized, with maximum proton conductivities reaching a value of 0.05S/cm for the doped porous membrane containing 70% porogen, compared to 1.5mS/cm obtained for dense membranes at room temperature. Another study [49] reported the preparation of porous PBI membranes using of glucose and saccharose as porogens in a solvent casting/porogen leaching method. A maximum conductivity of 34mS/cm was reported with porous PBI membranes having upto 15.7 mols H_3PO_4 per PBI unit. Chen et al.[100] reported the synthesis of porous PBI membranes for Direct Borohydride Fuel Cell applications using water-vapour phase inversion process. Membranes prepared were chemically stable, selectively permeable to the transport of hydroxyl ions across the membrane and discharged at 200mA/cm^2 for over 250 hours without voltage decay. Modifications of porous PBI membranes with combinations of dense and porous membranes[101] and functionalized fillers[ref] to further enhance properties have also been reported.

Although many instances of porous PBI membranes have been reported, porous ABPBI membranes are scant in literature. Zheng et. al. [76] have reported the preparation of porous ABPBI membranes with using Sodium Dodecyl Sulfate as a template, achieving proton conductivity values twice than that of the dense ABPBI at 180oC under dry conditions. Ulhas et. al. [102] has also reported the synthesis of structurally stable porous ABPBI. Other than this, there has been no other report of porous ABPBI to the best of our knowledge.

5. MEMBRANE CHARACTERISATION AND ANALYSIS

A polymeric membrane meant for HT-PEMFC application is required to meet certain physico-chemical standards. Base membranes are modified structurally (by incorporation of crosslinkers, porogens, etc.) or chemically (by introduction of organic and/or inorganic composite materials) in order to enhance its properties to meet these standards better. The following are some of the few methods used to estimate membrane properties.

5.1. Structural Analysis:

5.1.1. Spectroscopic Studies:

The polymeric backbone in both its protonated and non-protonated states has been investigated using Fourier Transform-Infra Red (FT-IR) Spectroscopy, Raman spectroscopy and nuclear magnetic resonance (NMR) Spectroscopy. Table 2. 1. shows the assignments for transmission bands for polybenzimidazole backbones as obtained from reports by Musto et al. [103] and others. [104-105] For ABPBI, the spectra is almost identical to that for PBI, with minor changes due to the nature of the polymeric backbone. Typically, the pristine polybenzimidazole exhibits a broad band stretching in the region of 4000 to 2000cm^{-1}. The relatively sharp peak centred at 3415cm^{-1} is reportedly due to the stretching of the non-bonded, isolated N–H groups in the imidazole, while that around 3145cm^{-1} is due to the hydrogen bonded, self-associated N···H bonds. These bands get further broadened in the presence of moisture.

Wave Number (cm^{-1})		
PBI	**ABPBI**	**Band Assignments**
3415	3392	Free, isolated N-H stretching
3145	3177	Associated, Hydrogen bonded N-H stretching
1614	1630	C=C/C=N stretching
	1547	Ring Vibration Characteristic of conjugation between benzene and imidazole ring
1285	1285	Breathing mode of imidazole ring

Table 2.1. Infra-Red Spectra of Polybenzimidazoles [103-105]

On doping with phosphoric acid, the protonation of the nitrogen of the imide group by one or more protons from the acid, leads to the appearance of a very broad absorption band complex in the wave number range from about 3000 to 2400cm^{-1}, [104-105]. As reported earlier by Glipa[105] the spectrum of phosphoric acid-doped PBI presents one region around 1250-750 cm^{-1} and one at 500 cm^{-1} that concentrates the main absorption bands of phosphoric acid and phosphates. With increase in doping levels, the intensity of this new band complex increases. Asensio et al. reported[102] the appearance of the C=C and C=N stretching in the region of 1630-1430cm^{-1} while the "breathing mode" of the imidazole ring appeared around 1285cm^{-1} for both polymers.

Litt et al. [106] used X-Ray Diffraction patterns to reveal the low crystallinity of the PBI polymers. Due to a plasticizing effect of the acid, the residual crystalline order was completely lost on doping with phosphoric as indicated by substantial decrease in Tg [107]. Using 1H and 31P magic-angle spinning NMR, Hughes et al. [107] investigated the polymer – acid interaction asserting the presence of four different 31P environments, i.e. bound and unbound phosphoric acid molecules (H_3PO_4) and acid anion ($H_2PO_4^-$), implying that protonation of imidazole rings occured by the hydrogen bonding of both H_3PO_4 and $H_2PO_4^-$.

5.1.2. Molecular weight determination.

The dependence between the intrinsic viscosity and the molecular weight of a polymer as given by the Mark-Houwink Sakurada equation is[108]:

$$[\eta] = K.M_v^a \qquad (3.1)$$

Where K and α are parameters related to the solvent, polymer and the temperature and Mv is the molecular average viscosity weight of the polymer.

The value of α ranges from 0.5-0.8, depending upon the configuration that the polymer molecule takes while in solution (larger the value, better the solvent). However, this equation does not apply to polymers with low molecular weights.

Intrinsic viscosity is defined as the limiting value of the ratio of the solution's specific viscosity to the concentration of the solute as the concentration approaches zero. According to Flory's proposition, this is an indication of the capacity of a polymer in a solution to increase the viscosity of the solutionby virtue of the average interactions of the polymer molecule with the solvent. Mathematically, this is represented as:

$$[\eta] = \lim \frac{\eta sp}{c} = \lim \frac{\eta r - 1}{c} \tag{3.2}$$

Where, η_{sp} = specific viscosity, defined as:

$$\eta_{sp} = \eta_r - 1 \tag{3.3}$$

η_r = relative viscosity, defined as:

$$\eta_r = \eta_{polyer\ solution} / \eta_{solvent} \tag{3.4}$$

and, c is concentration of the polymeric solution.

As per Poisueille's law, the time of flow of a polymer solution through a thin capillary should be proportional to the viscosity of the solution and inversely proportional to its density. i.e.

$$t_{solvent} = \eta_{solvent} / \rho_{solvent} \tag{3.5}$$

$$t_{solution} = \eta_{solution} / \rho_{solution} \tag{3.6}$$

At low polymer concentrations, the density of the polymeric solution is almost the same as that of the solvent used. Thus, viscosities may be directly obtained as a ratio of the times of flow of the solution and the solvent down the capillary of the viscometer. Using equations 1-5, relative and specific viscosities are then defined as:

$$\eta_r = t_{polyer\ solution} / t_{solvent} \tag{3.7}$$

$$\eta_{sp} = t_{polyer\ solution} / t_{solvent} - 1 \tag{3.8}$$

Viscometers used for the purpose are generally Ubbelohde viscometers with an additional pressure equilibration duct as compared to Cannon–Fenske viscometers. Most common unit for expressing [η] values is dl/gm.

5.1.3. Microscopic Imaging:

SEM TEM and AFM micrographs allow the morphological study of surfaces and cross sections of the polybenzimidazole membrane. Krishnan et al.[109] reports that while the top surface of the ABPBI membrane (surface from which evaporation takes place) has roughness and appears dull in nature, the face adjacent to the glass appears smooth and shiny. This discrepancy, along with presence of occasional pinholes and aggregates suggests that the membrane formation goes through an improper phase change. In case of composite membranes, SEM images reveal the presence of possible agglomerates[110], as well as discrepancies in phase separation [111] . Presence of pores in the polymer matrix is also readily recognisable as reported extensively in the literature [112-115]. It is possible to make some prediction of the types of pores and their distribution as seen from these images.

5.1.4. Water Uptake:

The polybenzimidazole backbone is highly hygroscopic due to the intermolecular hydrogen bondings between water molecules and the nitrogen and N–H sites[116-117]. The presence of a hydrophilic domain leads to better water uptake and consequently aids proton hopping [118]. At a given temperature and relative humidity, the water uptake capacities of the polymeric membranes are dictated by the pre-treatment[119] and elasticity and of the matrix along with the dissociation constant and number of conducting groups[120].

Percentage water uptake by the membrane sample post immersion in deionized water for a suitable period of time, maybe measure by the following equation[121]:

$$\text{Water uptake}\,(\%) = \left[\frac{W_{\text{wet}} - W_{\text{dry}}}{W_{\text{dry}}}\right] \times 100\% \qquad (3.9)$$

where, W_{dry} is the weight of the membrane sample after vacume drying and W_{wet} is the weight of the saturated membrane.

On absorption of moisture, the polymeric membranes swell due to the hydration of the hydrophilic domains. A substantial water uptake may be beneficial towards increasing proton conductivities, but may cause damage to the Membrane Electrode Assembly due to excessive swelling, culminating in lowered fuel cell performances [J Mater Chem, 2012, 22, 18550-18557][J Membr Sci, 2011, 367, 265-272] Therefore, it is desirable to have a PEM with a high proton conductivity that undergoes negligible changes in volumes during hydration and dehydration cycles.[Chem Rev, 2004, 104, 4587-4612] Water uptake capacities may be enhanced by the introduction of hygroscopic fillers (silica based composites) or by the introduction of pores within the matrix. The pores are expected to capture and retain more water molecules due to capillary action. However, this advantage comes at the cost of reduced mechanical strengths.

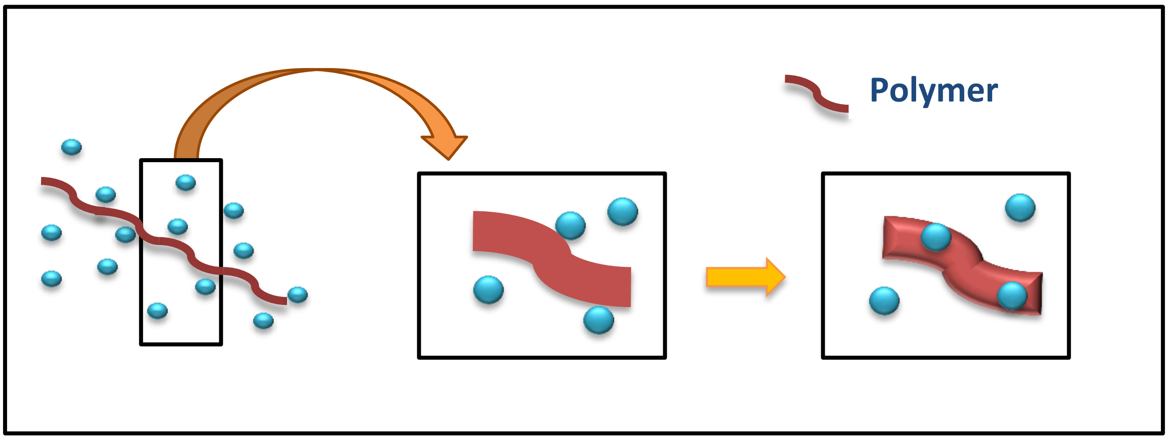

Fig 2.5. Schematic representation of water uptake and consequent swelling for ABPBI

5.1.5. Acid Uptake:

Polybenzimidazole based membranes are basic in nature with a pKa value of 5.23 as protonated[122]. Thus they react spontaneously with a strong acid. Inorganic acids like HBr [104-105], H_2SO_4 [104-105,123-125], $HClO_4$ [124], HNO_3 [124], HCl [124], H_3PO_4 [104-106,124-127], has been investigated as suitable dopants. Organophosphonic acids have also been examined as dopants to improve acid retaining properties [129]. Also, high acid-doping levels have been reportedly achieved via the TFA casting method.

Amongst these, phosphoric acid with both acid and basic groups, is of special interest. Low vapour pressures at elevated temperatures and excellent thermal stability makes it suitable as a dopant acid as compared to other mineral acids. On immersion in an aqueous acid bath (60-70%), equilibrium acid contents are reached roughly within 3-5 days, where it has been observed that the active sites of the imidazole rings are preferably occupied by acid molecules compared to water molecules[116]. Further doping in the acid may result in degeneration of the polymer matrix, based on the molecular weight of the polymer and modifications introduced into the membranes.

The acid uptake percentage of a membrane maybe given as[116]:

$$\text{Acid Uptake \%} = \frac{\textbf{Wdoped} - \textbf{Wundoped}}{\textbf{Wundoped}} * 100\% \qquad (3.10)$$

Where, $W_{\mathbf{undoped}}$ and $W_{\mathbf{doped}}$ are the weight of dried membrane before and after doping with acid, respectively.

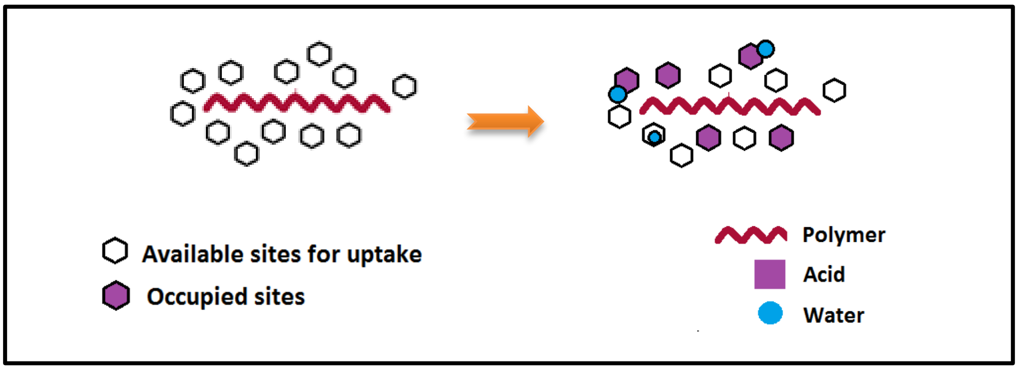

Fig. 2.6. Schematic representation of acid doping process for ABPBI

The doping chemistry of Polybenzimidazole membranes was elucidated by He et al. using the Scatchard method[129]. Under the consideration that the acid remains distributed between the aqueous phase and the polymer immersed in the solution, it was suggested that there are two types of polymer sites for the acid doping, one with a higher affinity than the other. The two types of dissociation constants associated with these two types of sites (S1 and S2) were found as[22]:

$$S1\text{-}H_3PO_4 \leftrightarrow S1+H^++H_2PO_4^- \qquad K^{a1}_{\mathbf{S1\text{-}H3PO4}} = 5.4\times10^{-4} \qquad (3.11)$$

$$S2\text{-}H_3PO_4 \leftrightarrow S2+H^++H_2PO_4^- \qquad K^{a1}_{\mathbf{S2\text{-}H3PO4}} = 3.6\times10^{-2} \qquad (3.12)$$

i.e. about one order smaller than that of aqueous phosphoric acid in the first case but 5 times higher in the second. Thus the acid absorbed at the second type of PBI sites with a larger dissociation constant, contributes most towards the proton hopping mechanism. With the introduction of pores within the membrane matrix, there would be a further accumulation and retention of acid due to capillarity. According to Weber et al.[34], this is again a two-step process involving a fast pore filling step due to capillary action, followed by a slower diffusion step involving movement of acid into pore walls to protonate the imidazole moieties.

5.1.6. Ion exchange capacity

The concentration of the ion conducting units is usually given by the measure of molar equivalents of ion conductor per mass of dry membrane and is expressed as ion exchange capacity (IEC) or mass specific milliequivalents of ion (meq/g or mmol/g) of polymer.

The ion exchange capacities maybe determined by back-titration method[130]. In this method, membranes in acid form were immersed in 1 M NaCl solution at 90°C for 24 h to exchange the H^+ ions for Na^+ ions. The H^+ ions were then titrated with NaOH aqueous solution of suitable strength using phenolphthalein as indicator. The titrated IEC of membrane was determined by[130]:

$$\mathbf{IEC = V_{NaOH} \times C_{NaOH} / W_{dry}} \qquad (3.11)$$

where, V_{NaOH} is the volume and C_{NaOH} is the concentration of NaOH, respectively. Wdry is the dry weight of membrane in the H^+ form.

The IEC value then gives an estimate of the number of replacable proton sites within the matrix, as well as their ease of detachment from the polymer chain.

5.1.7. Thermal Stability:

Thermal Analysis (TA) is a set of techniques used to study the properties of materials as they change with temperature. Thermal analysis maybe used to give gives properties like enthalpy, thermal capacity, mass changes and the coefficient of heat expansion. There are several techniques which are distinguished from each other by the specific property that it measures. Some of these are:

- Thermogravimetric analysis (TGA) – mass difference
- Differential thermal analysis (DTA) - temperature difference
- Differential scanning calorimetry (DSC) - heat difference

Therogravimetric analysis gives an estimation of mass changes of the sample with temperature due to various physical (gas adsorption/desorption, phase transitions) and chemical (decomposition, reactions with gasses, chemisorption) phenomena. A derivative weight loss curve can be used to tell the point at which weight loss is most apparent. Thus, characterization of thermal stabilities, moisture content and presence and effect of foreign materials on known samples may be carried out using this method. Absolute estimation of decomposition processes is possible when exit gasses are studied (eg. by gas chromatography).

TGA of ABPBI has been carried out extensively. Typically, pristine ABPBI loses 10-15% weight at temperatures below 150^{o}C in the form of absorbed water [121,132]. Consequently there is no significant weight loss till temperatures over 500^{o}C, where the matrix starts to degenerate. Acid doped membranes, additional weight losses due to dehydration of phosphoric acid and pyrophosphoric acid were observed around 200^{o}C[33]. During fuel cell operation, this loss of dopant acid would lead to reduced conductivity and hence, reduced cell performances. Complete disintegration occurs around 800^{o}C [121,132-133].

In case of porous membranes, the matrix is reported to suffer a greater weight loss as compared to the pristine Polybenzimidazole at temperatures below 200^{o}C[134]. This is indicative of the fact that higher amounts of un-vaporised moisture remained within the capillaries of the porous membranes. The general degradation curves were of similar patterns, indicating excellent thermal stabilities within the working conditions of the fuel cell. For benzyl-methyl-phosphoric acid grafted PBI[135], the grafted hydrophilic benzyl-methyl-phosphoric acid side chains caused the composite membrane to possess a higher moisture content than the pristine PBI membrane.

5.1.8. Oxidative Stability:

Under the operating conditions of a HT-PEMFC, the hydrogen peroxide and $HO^{\bullet}$ and $HOO^{\bullet}$ radicals formed from its decomposition attack the polymer electrolytic membrane, thereby oxidising it. This contributes towards the maximum degradation of the polymeric membrane while use in the PEMFC which is enhanced with the increase in temperatures. The ability to resist the peroxy radical induced chemical degradation gives the oxidative stability of the membrane[136]. Thus, one of the main challenges of making suitable ABPBI based membranes for PEMFC applications is to enhance their oxidative stabilities.

Experimental simulation of the process conditions is possible by generating the $HO^{\bullet}$ and $HOO^{\bullet}$ radicals artificially. This may be done by the catalysis of H_2O_2 in presence of Fe^{2+}/Fe^{3+}, a method termed as the Fenton's test used for the stability evaluation of PEMFC membranes [136]. By immersing membrane samples in a 3% H_2O_2 aqueous solution containing 4 ppm Fe^{2+} at 80°C and studying weight losses periodically, an estimate of oxidative degradation of the membrane within the fuel cell may be made.

In comparison to perfluorinated PEM, aromatic polymers such as ABPBI based PEMs exhibit inferior resistance to oxidation due to the presence of the benzene ring that possesses a high electron density [101]. Gaudiana and Conley [138] suggested that the initial stages of oxidative attack to benzimidazoles occur preferentially at the aromatic rings bearing the nitrogen containing functional group and subsequently the amine portion of the molecules. That is, the nitrogen containing heterocyclic and adjacent benzenoid rings are the weak links in the polymer backbone. Ionic and covalent cross-linking of the polymer can be achieved by an amide-type linkage through its imidazole rings. This has proved to be an effective way to improve the stability of the aromatic heterocyclic polymers. [139-140]. Addition of CeO_2 in the form $Cs_xH_{3-x}PW_{12}O_{40}/CeO_2$ nanoparticles has been reported to increase the oxidative stability of ABPBI as much as 75% where the CeO_2 behaved as free radical scavengers [100]. In case of porous polymeric matrix, however, larger exposed surface areas for free radical attack have resulted in lower oxidative stabilities for the membranes [141].

5.1.9. Mechanical Stability:

The mechanical strength of polybenzimidazole is directly related to the degree of polymerisation. It has been reported that with an increase of average molecular weight from 20,000 to 55,000g/mol, mechanical strength of acid doped PBI membranes increase three fold [142]. The strong hydrogen bonding between N and –NH– groups in polybenzimidazole matrix is the predominant molecular force, which results in close chain packing, thus allowing high mechanical strengths. On introduction of phosphoric acid, the polymer chains suffer a decrease in molecular cohesion. On the other hand, there are new hydrogen bonds formed between the basic sites of the polymer and the incoming acid. These two contradicting effects nullify each other at low concentrations of acid (doping levels less than 2) and no substantial change in mechanical properties is observed [106,122]. However, when doping levels are higher and the number of available basic sites is less than the number of acid molecules present, the free acid hinders intermolecular attractions within the polymer matrix and hence decreases mechanical strength. This effect is relatively less prominent in polymers with extremely high degrees of polymerisation [143-144] or crosslinking[145-146], where the polymer backbone is too tightly wound for the free acid to have significant effect. Introduction of fillers also has effects on the polymeric membrane. Introduction of POSS incorporated ionic liquids into the polymer matrix resulted in an 18% increase in tensile strength in the composite membrane, with the elongation at break coming down to almost one-third of the value for the pure ABPBI membrane [147]. While a good dispersion of the fillers increased tensile strength, the ionic liquid and POSS particles inhibited polymer chain movement, making it brittle.

5.2. Proton Conductivity :

An excess proton introduced into the polymer matrix acts as a “defect”. The propagation of this “defect” along the polymer chain constitutes the proton conduction mechanism. As per Grotthuss’ theory, hydrogen bonds networks of water molecules, polymer backbones and other fillers if present, form, cleave and reform in a constant cycle; each basic site simultaneously accepts and passes to the next one an excess proton in a “bucket line” manner [148-150]. The excess proton is believed to exist in one of the two following possible forms[151]:

a. Eigen cation ($H_9O_4^+$) – a hydrated hydronium ion

b. Zundel cation ($H_5O_2^+$) – a dimer

There is thermodynamic stability between the two forms, and as such the protons may exist in either form with equal probability. [151-152]

In case of membranes meant for high temperature PEMFC application, the acid environment acts as a solvent for in diffusion. Bouchet et. al. [104] reported conductivities of acid-doped PBI membranes under dry conditions. It was suggested that the proton hops from one imide site to the next vacant one, assisted by a counter anion with the Grotthuss mechanism[104,122] Bound and unbound phosphoric acid molecules as well as acid anions ($H_2PO_4^-$) present in the doped PBI matrix participate in the Grotthuss mechanism[107]. The hydrogen bonding between free acid molecules has also been observed. Ma et al. [127] has proposed the following order of the rate of proton transfer between various species:

H_3PO_4 to H_2O > H_3PO_4 to $H_2PO_4^-$ > $N–H^+$ to $H_2PO_4^-$ > $N–H^+$ to H_2O > $N–H^+$ to $N–H$.

At acid doping levels below 2, the phosphoric acid molecules donate a proton to the available basic sites and remain bound to the polymer matrix. Proton conductivity studies for membranes with low acid doping levels under hydrated[126] and anhydrous states[104,123] have revealed low values of proton transfer, indicating efficient conduction is only possible in the presence of excess free acid, that is at higher doping levels. At higher doping levels of 4–6, the proton hopping occurs mainly along the acid and anion chain ($H_2PO_4^- – H^+– H_2PO_4^-$) or the acid and water chain ($H_2PO_4^-–H^+\cdot\cdot\cdot H_2O$) depending on the moisture content[27]. The proton conductivity measurements are taken using two probe or four probe methods.

5.3. Fuel Cell Performance Studies :

Fuel Cell testing is usually carried out to study different performance behaviour viz. changes in cell voltage with changes in fuel cell load (current or current density) and vice versa or amount of power that may be drawn from the fuel cell. Fuel cell tests may be carried out by three different ways[153]:

i. **Current control mode** : Cell voltage changes are studied with controlled changes in current (or current density) to obtain I-V curves.
ii. **Voltage control mode** : Current or Current density changes are studied with controlled changes in cell voltage to obtain I-V curves.
iii. **Power control mode** :

Power densities obtained from fuel cell IV curves may be represented in three ways[53]:

i. **MEA power density** : Power obtained from a single fuel cell per unit area of the MEA (Watts/cm^2).
ii. **Mass specific stack power density** : Power obtained from a stack fuel cell per unit mass of the stack (Watts/kg).
iii. **Volume specific stack power density** : Power obtained from a stack fuel cell per unit volume of the stack (Watts/L).

Apart from maximum power densities obtainable, durability tests aimed at determining the lifetime of a fuel cell is also important parameter. During continued usage for a prolonged duration of time (a minimum of a year), the Beginning of Lifetime (BOL) and End of Lifetime (EOL) tests are carried out, recording I-V polarization curves. The differences between two voltages at a given current density is estimated from the two curves, and reported as a function of time.

Generally, the fuel cell performance is a function of temperature, pressure, thermo-oxidative and mechanical stabilities, relative humidity and reactant gas stoichiometry. Apart from this, structural modifications of the polymer electrolyte membranes play a vital role in the nature of the IV curves obtained. For ABPBI/ Cs_xH_3-$xPW_{12}O_{40}/CeO_2$ composite membranes reported power densities were up to 530mW/cm^2, an 18% increase from that reported for the pristine ABPBI[110].

5.4. Pore Property Characterizations:

Surface imaging techniques viz. SEM, TEM and AFM allow the estimation of surface topography, and give a preliminary idea about the surface pore morphology [156-157]. However, in order to determine properties like pore volume, presence of embedded pores and pore interconnectivity, further analysis is required. While methods like liquid displacement are relatively simpler methods that give an idea of overall pore volume, sophisticated techniques like Intrusion Porosimetry allow the determination of total pore size distributions, pore volumes and pore tortuosity.

❖ Porosimetry Method

Pore volumes and pore size distribution can be well understood using Intrusion Porosimetry Techniques. Two main types of intrusion methods are used to characterise the distribution of pores within a polymer matrix. N_2 intrusion porosimetry is a non-destructive method used for the detection of micro and meso pores (seldom macro pores) [156,158-161] while Hg intrusion porosimetry is a destructive method aimed at determining the presence of meso and macro pores [157-159,161,163]. This is directly attributable to the lower molecular weight of the gas and its consequent ability to penetrate into small pores as compared to mercury. Thus, appropriate estimation should be made before choosing either method, or in case of doubt, both methods should be used concurrently. Both methods give an estimation of total pore volume while BET studies using N2 sorption isotherm give the surface area. About 300g of material is required in order to give reproducible data in either case.

❖ Fluid Saturation Method

Intrusion Porosimetry methods primarily involve backfilling the sample with a suitable fluid, and hence, may fail when there are pores embedded within the polymer matrix that do not open onto the surface. This problem may be bypassed by the solvent uptake method. In this process, a non-reactive solvent like heptane, methanol, toluene, butanol, etc. of known density is used to saturate the membrane sample, which is then weighed. The difference between the dry and saturated weights gives a measure of the pore volume[164].

REFERENCE

1. Wainright JS, Wang JT, Weng D, Savinell RF, Litt M. Acid-doped polybenzimidazoles—a new polymer electrolyte. J Electrochem Soc 1995;142:L121–3.
2. Savinell RF, Litt MH. Proton conducting polymers used as membranes (Case Western Reserve University). US patent 5,525,436 (1996).
3. Savinell RF, Litt MH. Proton conducting polymers prepared by direct acid casting (Case Western Reserve University). US patent 5,716,727 (1998).; (b) Savinell RF, Litt MH. Proton conducting solid polymer electrolytes prepared by direct acid casting (Case Western Reserve University). US patent 6,025,085 (2000).; (c) Savinell RF, Litt MH. Proton conducting polymers prepared by direct acid casting (Case Western Reserve University). US patent 6,099,988 (2000).
4. (a) Sansone MJ, Onorato FJ, Ogata N. Acid-modified polybenzimidazole fuel cell elements (Hoechst Celanese Corporation). US patent 5,599,639 (1997).;
5. (b) Yamamoto T. Method for producing bridged polymer membrane and fuel cell (Celanese Ventures GmbH). US patent 6,790,553 (2004).; (c) Onorato FJ, Sansone MJ, French SM, Marikar F. Process for producing polybenzimidazole pastes and gels for use in fuel cells (Aventis Research & Technologies GmbH & Co. KG). US patent 5,945,233 (1999).; (d) Onorato FJ, Sansone MJ, Kim DW, French SM, Marikar F. Process for producing polybenzimidazole fabrics for use in fuel cells (Aventis Research & Technologies GmbH & Co. KG). US patent 6,042,968 (2000).; (e) Sansone MJ, Onorato FJ, French SM, Marikar F. Process for producing polymeric films for use as fuel cells (Celanese Ventures GmbH). US patent 6,187,231 (2001).
6. (a) Akita H, Ichikawa M, Nosaki K, Oyanagi H, Iguchi M. Solid polymer electrolytes (Honda). US patent 6,124,060 (2000).;(b) Oyanagi H, Sato S, Ise M, Okamoto T. Method of operating phosphoric acid fuel cell (Honda). US patent 6,833,204 (2004).; (c) Okamoto T, Okazaki K, Sato S. Fuel cell system (Honda). US patent 6,815,109 (2004).
7. (a) Li C, Lian KK, Eschbach FO. Electrochemical cell having a polymer electrolyte (Motorola, Inc.). US patent 5,688,613 (1997).; (b) Wu H, Li C, Lian KK. Polymer electrolyte and an electrochemical cell containing the electrolyte (Motorola, Inc.). US patent 5,723,231 (1998).
8. Bjerrum NJ, Li Q, Hjuler HA. Polymer electrolyte membrane fuel cells (Danish Power Systems). US patent 6,946,211 and EP 1,523,053 (2002).

9. (a) Huang WW. Integrated fuel cell system (Plug Power Inc.). US patent 6,753,107 (2004).; (b) Ingraham JE, Cutright, Richard H. Integrated fuel cell system (Plug Power Inc.). US patent 6,913,846 (2005)
10. Bouchet R, Siebert E. Proton conduction in acid doped polybenzimidazole. Solid State Ionics 1999;118:287–99.
11. Glipa X, Bonnet B, Mula B, Jones DJ, Roziere J. Investigation of the conduction properties of phosphoric and sulfuric acid doped polybenzimidazole. J Mater Chem 1999;9:3045–9.
12. Kawahara M, Morita J, Rikukawa M, Sanui K, Ogata N. Synthesis and proton conductivity of thermally stable polymer electrolyte: poly(benzimidazole) complexes with strong acid molecules. Electrochim Acta 2000;45:1395–8.
13. He RH, Li QF, Xiao G, Bjerrum NJ. Proton conductivity of phosphoric acid doped polybenzimidazole and its composites with inorganic proton conductors. J Membr Sci 2003;226:169–84.
14. Ma YL, Wainright JS, Litt MH, Savinell RF. Conductivity of PBI membranes for high-temperature polymer electrolyte fuel cells. J Electrochem Soc 2004;151:A8–16
15. Samms SR, Wasmus S, Savinell RF. Thermal stability of proton conducting acid doped polybenzimidazole in simulated fuel cell environments. J Electrochem Soc 1996;143:1225–32.
16. M. Kawahara, J. Morita, M. Rikukawa, K. Sanui and N. Ogata, Electrochim. Acta, 2000, 45, 1395–1398.
17. L. Xiao, H. Zhang, T. Jana, E. Scanlon, R. Chen, E. W. Choe, L. S. Ramanathan, S. Yu and B. C. Benicewicz, Fuel Cells, 2005, 5, 287–295.
18. Suryani and Y. L. Liu, J. Membr. Sci., 2009, 332, 121–128. 11 A. D. Modestov, M. R. Tarasevich, V. Y. Filimonov and N. M. Zagudaeva, Electrochim. Acta, 2009, 54, 7121–7127.
19. S. Yu, L. Xiao and B. C. Benicewicz, Fuel Cells, 2008, 3–4, 165– 174.
20. L. Xiao, H. Zhang, E. Scanlon, L. S. Ramanathan, E. W. Choe, D. Rogers, T. Apple and B. C. Benicewicz, Chem. Mater., 2005, 17, 5328–5333.
21. K. D. Kreuer, A. Fuchs, M. Ise and M. Spaeth, Electrochim. Acta, 1998, 43, 1281–1288. 15 D. J. Jones and J. Roziere, J. Membr. Sci., 2001, 185, 41–58.
22. Li QF, He RH, Gao JA, Jensen JO, Bjerrum NJ. The CO poisoning effect in PEMFCs operational at temperatures up to 200 ◦C. J Electrochem Soc 2003;150:A1599–605.
23. Wang JT, Savinell RF, Wainright JS, Litt M, Yu H. A H2/O2 fuel cell using acid doped polybenzimidazole as polymer electrolyte. Electrochim. Acta, 1996;41:193–7.

24. Jensen JO, Li Q, He R, Pan C, Bjerrum NJ. 100–200 oC polymer fuel cells for use with NaAlH4. J Alloys Compd 2005;404–406:653–6.
25. Jensen JO, Li QF, Pan C, Vestbo AP, Mortensen K, Petersen HN, et al. High temperature PEMFC and the possible utilization of the excess heat for fuel processing. Int J Hydrogen Energy 2007;32:1567–71.
26. Vogel H, Marvel CS. Polybenzimidazoles, new thermally stable polymers. J Polym Sci 1961;50:511–39.
27. Neuse EW. Aromatic polybenzimidazoles—syntheses, properties and applications. Adv Polym Sci 1982;47:1–42.
28. Choe EW. Catalysts for the preparation of polyb enzimidazoles. J Appl Polym Sci 199 4;53:4 97–50 6.
29. Choe EW. Single-stage melt polymerization process for the production of high molecular weight polybenzimidazole (Celanese Corporation). US patent 4,312,976 (19 82)
30. Iwakura Y, Imai Y, Uno K. Polyphenylenebenzimidazoles. J Polym Sci Part A 1964;2:2605–15.
31. Xiao LX, Zhang HF, Scanlon E, R amanathan L S, Choe EW, Rogers D, et al. High-temperature polyb enzimidazole fuel cell membranes via a sol–gel process. Chem Mater 20 05;17:5328–33.
32. Xiao L, Zhang H, Jana T, Scanlon E, Chen R, Choe EW, et al. Synthesis and characterization of pyridine-base d polyb enzimidazoles for high temperature polymer electrolyte membrane fuel cell applications. Fuel Cells 20 05;5:287–95.
33. Kim JH, Kim HJ, Lim TH, Lee HI. Dependence of the performance of a high-temperature polymer electrolyte fuel cell on phosphoric acid-doped polybenzimidazole ionomer content in cathode catalyst layer. J Power Sources 2007;170:275–80.
34. Wainright JS, Litt MH, Savinell RF. High temperature membranes. In: Vielstichm W, Lamm A, Gasteiger HA, editors. Handbook of fuel cells, vol. 3. John Wiley & Sons Ltd.; 2003. p. 436–46.
35. Li Q., Jensen J.O., Savinell R., Bjerrum N.J. High temperature proton exchange membranes based on polybenzimidazoles for fuel cells. J. Progress in Polymer Science 34 (2009) 449–477
36. Bose S., Kuila T., Nguyen T., Kim N. H., Lau K., Lee J.H. Polymer membranes for high temperature proton exchange membrane fuel cell: Recent advances and challenges. J. Progress in Polymer Science 36 (2011) 813–843
37. Carollo A , Quartarone E, Tomasi C, Mustarelli P, Belotti F, Magistris A et al. Developments of new proton conducting membranes based on different

polybenzimidazole structures for fuel cells applications. J Power Sources 2006;160:175–80.

38. Li QF, Jensen OJ. Membranes for high temperature PEMFC based on acid-doped polybenzimidazoles. In: Peinemann KV, Nunes SP, editors. Membranes for energy conversion, vol. 6. Wiley-VCH; 20 07. p. 61–96.
39. Qing SB, Huang W, Yan DY. Synthesis and characterization of thermally stable sulphonate d polyb enzimidazoles. Eur Po ly m J 20 05;41:1589–95.
40. Kerres JA. Blended and cross-linked ionomer membranes for application in membrane fuel cells. Fuel Cells 2005;5:230–47
41. Zhang W, Gogel V, Friedrich KA, Kerres J. Novel covalently cross-linked poly(etheretherketone) ionomer membranes. J Power Sources 2006;155:3–12.
42. Kerres J. Covalent-ionically cross-linked poly(etheretherketone)- basic polysulphone blend ionomer membranes. Fuel Cells 2006;6:251–60.
43. Davis HJ, Thomas NW. Chemical modification of Polybenzimidazole semipermeable (Celanese Corporation). US patent 4,020,142 (1977).
44. Li Q, Pan C, Jensen JO, Noyé P, Bjerrum NJ. Cross-linked polybenzimidazole membranes for fuel cells. Mater Chem 2007;19:350–2.
45. Jones DJ, Roziére J. Inorganic/organic composite membranes. In:Vielstichm W, Lamm A, Gasteiger HA, editors. Handbook of fuel cells, vol. 3. John Wiley & Sons Ltd.; 2003. p. 447–63.
46. Ogoshi T, Chujo Y. Organic–inorganic polymer hybrids prepared by the sol–gel method. Compos Interf 2005;11:539–66.
47. Herring AM. Inorganic–polymer composite membranes for proton exchange membrane fuel cells. J Macromol Sci C: Polym Rev 2006;46:245–96
48. Mecerreye D., Grande H., Miguel O., Ochoteco E., Marcilla R., and Cantero I. Porous Polybenzimidazole Membranes Doped with Phosphoric Acid: Highly Proton-Conducting Solid Electrolytes. Chem. Mater. 2004, 16, 604-607
49. J. Li et al./Energy Conversion and Management 85 (2014) 323–327
50. Li-Cheng Jheng,ab Steve Lien-Chung Hsu,*a Tzung-Yu Tsaia and Wesley Jen-Yang Chang. J. Mater. Chem. A, 2014,2, 4225
51. Cheng-Hsun Shen, Li-cheng Jheng, Steve Lien-chung Hsu* and Jacob Tse-Wei Wang. J. Mater. Chem., 2011, 21, 15660
52. M. Litt, R. Ameri, Y. Wang, R. Savinell, and J. Wainwright, Mater. Res. Soc. Symp. Proc., 548, 313 (1999)
53. J.A. Asensio, S. Borro´s, P. Romero. Polymer Electrolyte Fuel Cells Based on Phosphoric Acid-Impregnated Poly(2,5-benzimidazole) Membranes. *Journal of The Electrochemical Society*, 151 (2) A304-A310 (2004).

54. J.A. Asensio, S. Borro´s, P. Romero. Proton-conducting membranes based on poly(2,5-benzimidazole) (ABPBI) and phosphoric acid prepared by direct acid casting. Journal of Membrane Science 241 (2004) 89–93.
55. P. Krishnan, J. Park, C. Kim. Performance of a poly(2,5-benzimidazole) membrane based high temperature PEM fuel cell in the presence of carbon monoxide. Journal of Power Sources 159 (2006) 817–823.
56. O. Acara, U.Sena, A. Bozkurtb, A. Ataa. Proton conducting membranes based on Poly(2,5-benzimidazole) (ABPBI)-Poly(vinylphosphonic acid) blends for fuel cells. Int. J. Hydrogen Energy. 34(2009) 2724 – 2730
57. W. Qian, Y. Shang, S. Wang, X. Xie*, Z. Mao. Phosphoric acid doped composite membranes from poly (2,5-benzimidazole) (ABPBI) and CsxH3L xPW12O40/CeO2 for the high temperature PEMFC. Int J Hydrogen Energy 2013;38; 11053-11059
58. J.A. Asensio, S. Borro´s, P. Romero. Sulfonated poly(2,5-benzimidazole) (SABPBI) impregnated with phosphoric acid as proton conducting membranes for polymer electrolyte fuel cells. Electrochimica Acta 49 (2004) 4461–4466.
59. T. Ko, K. Kim, M.Y. Lim, S.Y. Nam, T.H. Kim, S.K. Kima, J.C. Lee. Sulfonated poly(arylene ether sulfone) composite membranes having poly(2,5-benzimidazole)- grafted graphene oxide for fuel cell applications. J. Mater. Chem. A, 2015,3, 20595.
60. P. Romero, J.A. Asensio, S. Borr´os. Hybrid proton-conducting membranes for polymer electrolyte fuel cells Phosphomolybdic acid doped poly(2,5-benzimidazole)—(ABPBI-H3PMo12O40). Electrochimica Acta 50 (2005) 4715–4720
61. F.Zhang, X.Bao, Q.Liu1, M.Huang. High Temperature Polymer Electrolyte Membranes Based on Poly(2,5-benzimidazole) (ABPBI) and POSS Incorporated Ionic Liquid. J. of Materials and Chemical Engineering. Oct. 2014, Vol. 2 Iss. 4, PP. 86-93.
62. J. Kang, S. Eo, I. Jeon, Y. Suk Choi, L. Tan, J. Baek. Multifunctional Poly(2,5-benzimidazole)/Carbon Nanotube Composite Films. Journal Of Polymer Science: Part A: Polymer Chemistry DOI 10.1002/POLA
63. B. Eren, R. Aydin, E. Eren. Morphology and thermal characterization of montmorillonite/ polybenzimidazole nanocomposite. J Therm Anal Calorim (2014) 115:1525–1531 DOI 10.1007/s10973-013-3470-z.
64. M. Linlina, A.K. Mishra, N.H. Kimc, J.H. Leea. Poly(2,5-benzimidazole)–silica nanocomposite membranes for high temperature proton exchange membrane fuel cell. J. Membrane Science. 411– 412 (2012) 91– 98.

65. A.K. Mishra, N.H. Kimc, J.H. Leea. Effects of ionic liquid-functionalized mesoporous silica on the proton conductivity of acid-doped poly(2,5-benzimidazole) composite membranes for high-temperature fuel cells. J. Membrane Science 449 (2014) 136–145
66. S.K. Kim, T. Kim, J. Jung, J. Lee. Copolymers of Poly(2,5-benzimidazole) and Poly[2,20-(p-phenylene)-5,50-bibenzimidazole] for High-Temperature Fuel Cell Applications. J. Macromol. Mater. Eng. 2008, 293, 914–921
67. O. Acara, U.Sena, A. Bozkurtb, A. Ataa. Blend membranes from poly(2,5-benzimidazole) and poly(styrene sulfonic acid) as proton-conducting polymer electrolytes for fuel cells. J Mater Sci (2010) 45:993–998
68. S.K. Kim, T. Kim, J. Jung, J. Lee. Cross-linked poly(2,5-benzimidazole) consisting of wholly aromatic groups for high-temperature PEM fuel cell applications. Journal of Membrane Science 373 (2011) 80–88
69. S. Wang, F. Dong, Z. Li. Proton-conducting membrane preparation based on SiO2-riveted phosphotungstic acid and poly (2,5-benzimidazole) via direct casting method and its durability. J Mater Sci (2012) 47:4743–4749
70. U.Sen, O. Acar, A. Bozkurt, A. Ata. Proton Conducting Polymer Blends from Poly(2,5- Benzimidazole) and Poly(2-Acrylamido-2-methyl-1-propanesulfonic acid). J. Applied Polymer Science, Vol. 120, 1193–1198 (2011)
71. H. Zheng, H.Luo, M. Mathe. Proton exchange membranes based on poly(2,5-benzimidazole) and sulfonated poly(ether ether ketone) for fuel cells. Journal of Power Sources 208 (2012) 176–179.
72. S. Di, L. Yan, S. Han, B. Yue, Q. Feng, L. Xie, Jin Chen, Dongfang Zhang, Chao Sun. Enhancing the high-temperature proton conductivity of phosphoric acid doped poly(2,5-benzimidazole) by preblending boron phosphate nanoparticles to the raw materials. Journal of Power Sources 211 (2012) 161e168.
73. F. Dong, Z. Li, S. Wang, Z. Wang. Synthesis and characteristics of proton-conducting membranes based on cerium sulfophenyl phosphate and poly (2, 5-benzimidazole) by hot-pressing method. Int. J. Hydrogen Energy 36 (2011) 11068 – 11074
74. T Kim, T. Lim, Y.Park, K. Shin, J. Lee* Proton-Conducting Zirconium Pyrophosphate/ Poly(2,5-benzimidazole) Composite Membranes Prepared by a PPA Direct Casting Method. J. Macromol. Chem. Phys. 2007, 208, 2293–2302
75. H. Zheng, M. Mathe.. Enhanced conductivity and stability of composite membranes based on poly(2,5-benzimidazole) and zirconium oxide nanoparticles for fuel cells. Journal of Power Sources 196 (2011) 894–898.

76. H.Zheng, L. Petrikb, M. Mathea. Preparation and characterisation of porous poly(2,5benzimidazole) (ABPBI) membranes using surfactants as templates for polymer electrolyte membrane fuel cells. Int. J. Hydrogen Energy; 2010; 1 – 6.
77. Yamamoto, M.; Tabata, Y. Tissue engineering by modulated gene delivery. Adv. Drug Deliv. Rev. 2006, 58, 535–554.
78. Portner, R.; Nagel-Heyer, S.; Goepfert, C.; Adamietz, P.; Meenen, N.M. Bioreactor design for tissue engineering. J. Biosci. Bioeng. 2005, 100, 235–245.
79. Tarascon, J.-M.; Godz, A. S.; Schmutz, C.; Shokoohi, F.; Warren, P. C. Solid State Ionics 1996, 86-88, 49.
80. (a) Quartarone, E.; Muscarelli, P. J. Phys. Chem. B. 2000, 104 (48), 11460. (b) Saito, Y.; Kataoka, H.; Capiglia, C.; Yamamoto, H. J. Phys. Chem. B. 2000, 104 (9), 2189.
81. Zaidi, S. M.; Chen, S. F.; Mikhailenko, S. D.; Kaliaguine, S. J. New Mater. Electrochem. Syst. 2000, 3, 27.
82. Ishaug-Riley, S.L.; Crane-Kruger, G.M.; Yaszemski, M.J.; Mikos, A.G. Three-dimensional culture of rat calvarial osteoblasts in porous biodegradable polymers. Biomaterials 1998, 19, 1405–1412.
83. Harris, L.; Mooney, D.J.; Shea, L. Open pore biodegradable matrices. United States Patent, 6,797,738, September 28, 2004.
84. Zhou, Z.H.; Ruan, J.M.; Zou, J.P.; Zhou, Z.C. Synthesis of poly-L-Lactide for scaffold materials by melt-Solid polycondensation. Polym.-Plast. Technol. Eng. 2007, 46, 1195–1199.
85. Mooney, D.J.; Baldwin, D.F.; Suh, N.P. Novel approach to fabricate porous sponges of poly(D,L-lactic-coglycolic acid) without the use of organic solvents. Biomaterials 1996, 17, 1417–1422.
86. Schugens, C.; Maquet, V.; Grandfils, C. Polylactide macroporous biodegradable implants for cell transplantation II. Preparation of poly-lactide foams for liquid-liquid phase separation. J. Biomed. Mater. Res. 1996, 30, 449–461.
87. Nam, Y.S.; Park, T.G. Porous biodegradable polymeric microcellular foams by modified thermally induced phase separation methods. Biomaterials 1999, 20, 1783–1790.
88. Mikos, A.G.; Bao, Y.; Cima, L.G. Preparation of poly(glycolic acid) bonded fiber structure for cell attachment and transplantation. J. Biomed. Mater. Res. 1993, 27, 183–189.
89. Mooney, D.J.; Mazzoni, C.L.; Breuer, C. Stabilized polyglycolic acid fiber-based tubes for tissue engineering. Biomaterials 1996, 17, 115–124.

90. Park, A.; Wu, B.; Griffith, L.G. Integration of surface modification and 3D fabrication techniques to prepare patterned poly(L-lactide) substrates allowing regionally selective cell adhesion. J. Biomater. Sci. Polym. Edi. 1998, 9, 89–110.
91. Ortiz-Palacios, J.; Cardoso, J.; Manero, O. Production of macroporous resins for heavy-metal removal. I. Nonfunctionalized polymers. J. Appl. Polym. Sci. 2008, 107, 2203–2210.
92. Drake, R.; Dunn, R.; Sherrington, D.C.; Thomson, S.J. Optimisation of polystyrene resin-supported pt catalysts in room temperature, solvent-less, oct-l-ene hydrosilylation using methyldichlorosilane. Comb. Chem. High Throughput Scr. 2002, 5, 201–209.
93. Deleuzel, H.; Schultze, X.; Sherrington, D.C. Porosity analysis of some poly(styrene/ divinylbenzene) beads by nitrogen sorption and mercury intrusion porosimetry. Polym. Bull. 2000, 44, 179–189.
94. Verweij, P.D.; Sherrington, D.C. High-surface-area resins derived from 2,3-epoxypropyl methacrylate cross-linked with trimethylolpropane trimethacrylate. J. Mater. Chem. 1991, 1, 371–374.
95. Guettaf, H.; Iayadene, F.; Bencheikh, Z.; Rabia, I. Structure and properties of styerene-divinylbenzene-methylmethacrylateterpolymers-ii- effect of methylacrylate at different n-heptane 2-ethyl-1-hexanol diluent composition. Eur. Polym. J. 1998, 34, 241–246.
96. Hamid, M.A.; Naheed, R.; Fuzail, M.; Rehman, E. The effect of different diluents on the formation of n-vinylcarbazole-divinylbenzene copolymer beads. Eur. Polym. J. 1999, 35, 1799–1811.
97. Chao, A.-C.; Yu, S.-H.; Chuang, G.-S. Using nacl particles as porogen to prepare a highly adsorbent chitosan membranes. J. Membr. Sci. 2006, 280, 163–174.
98. Courtois, J.; Szumski, M.; Georgsson, F.; Irgum, K. Assessing the macroporous structure of monolithic columns by transmission electron microscopy. Anal. Chem. 2006, 79, 335–344.
99. Zhou, Z.; Liu, X.; Liu, Q. A comparative study of preparation of porous poly-l-lactide scaffolds using NaHCO3 and NaCl as porogen materials. J. Macromol. Sci. Part B 2008, 47, 667–674.
100. Chen, D.; Yu, S.; Liu, X.; Li, X.; Porous polybenzimidazole membranes with excellent chemical stability and ion conductivity for direct borohydride fuel cells. Journal of Power Sources 282 (2015) 323 - 327
101. Zeng, L.; Zhao, T. S.; An, L. ; Zhao, G. ; and X. H. Yan. A high-performance sandwiched-porous polybenzimidazole membrane with enhanced alkaline retention for anion exchange membrane fuel cells. Energy Environ. Sci., 2015, 8, 2768

102. US 2013/0053467 A1 . Feb. 28, 2013 . Ulhas Kharul, Pune (IN); Harshada Lohokare, Pune (IN). Porous Abpbi [Poly (2, 5-Benzimidazole)] Membrane And Process Of Preparing The Same.

103. Musto P, Karasz FE, Macknight WJ. Hydrogen-bonding in polybenzimidazole polyimide systems—a Fourier-transform infrared investigation using low-molecular-weight monofunctional probes. Polymer 1989; 30:1012–21.

104. Asensio J, Borro´s S and Romeroa P. Polymer Electrolyte Fuel Cells Based on Phosphoric Acid-Impregnated Poly(2,5-benzimidazole) Membranes. J. Electrochem Soc., 151 (2) A304-A310 (2004)

105. Ko T, Kim K, Lim M, Nam S, Kim T, Kima S and Lee J. Sulfonated poly(arylene ether sulfone) composite membranes having poly(2,5-benzimidazole)- grafted graphene oxide for fuel cell applications. J. Mater. Chem. A, 2015,3, 20595.

106. Bouchet R, Siebert E. Proton conduction in acid doped polybenzimidazole. Solid State Ionics 1999;118:287–99.

107. Glipa X, Bonnet B, Mula B, Jones DJ, Roziere J. Investigation of the conduction properties of phosphoric and sulfuric acid doped polybenzimidazole. J Mater Chem 1999;9:3045–9.

108. Litt M, Ameri R, Wang Y, Savinell R, Wainwright J. Polybenzimidazoles/phosphoric acid solid polymer electrolytes: mechanical and electrical properties. Mater. Res. Soc. Symp. Proc. 1999;548:313–23.

109. Hughes CE, Haufe S, Angerstein B, Kalim R, Mahr U, Reiche A, et al. Probing structure and dynamics in poly[2,2’-(m-phenylene)-5,5'- bibenzimidazole] fuel cells with magic-angle spinning NMR. J Phys Chem 2004;108:13626–31.

110. Wainright, J.; Litt, M.H.; Savinell, R.F. in Handbook of Fuel Cells, Fundamentals, Technology and Applications, Vol 3, John Wiley and Sons, New York, 2003.

111. Krishnan P, Park J, Kim C; Performance of a poly(2,5-benzimidazole) membrane based high temperature PEM fuel cell in the presence of carbon monoxide. Journal of Power Sources 159 (2006) 817–823

112. Wei Qian, Yuming Shang, Shubo Wang, Xiaofeng Xie*, Zongqiang Mao; Phosphoric acid doped composite membranes from poly (2,5-benzimidazole) (ABPBI) and $Cs_xH_{3-x}PW_{12}O_{40}/CeO_2$ for the high temperature PEMFC. Int. J. of Hydrogen Energy. 38 (2013) 11053 -11059.

113. Ff

114. Mecerreyes D, Grande H, Miguel O, Ochoteco E, Marcilla R and Cantero I. Porous Polybenzimidazole Membranes Doped with Phosphoric Acid: Highly Proton-Conducting Solid Electrolytes. Chem. Mater., Vol. 16, No. 4, 2004 605

115. Jin Li, Xiaojin Lia, Shuchun Yu, Jinkai Hao, Wangting Lu, Zhigang Shao, Baolian Yi. Porous polybenzimidazole membranes doped with phosphoric acid: Preparation and application in high-temperature proton-exchange-membrane fuel cells. Energy Conversion and Management 85 (2014) 323–327.
116. Dongju Chen, Shanshan Yu, Xue Liu, Xianfeng Li. Porous polybenzimidazole membranes with excellent chemical stability and ion conductivity for direct borohydride fuel cells. Journal of Power Sources 282 (2015) 323-327.
117. Haitao Zheng, Leslie Petrik, Mkhulu Mathe. Preparation and characterisation of porous poly(2,5benzimidazole) (ABPBI) membranes using surfactants as templates for polymer electrolyte membrane fuel cells. Int. J. of Hydrogen Energy. (2010) 1–6.
118. Li QF, He RH, Berg RW, Hjuler HA, Bjerrum NJ. Water uptake and acid doping of polybenzimidazoles as electrolyte membranes for fuel cells. Solid State Ionics 2004;168:177–85.
119. Brooks NW, Duckett RA, Rose J, Ward IM, Clements J. An NMR-study of absorbed water in polybenzimidazole. Polymer 1993;34:4039–42.
120. Jang W, Choi S, Lee S, Shul Y, Han H. Characterization and stability of polyimide–phosphotungstic acid composite electrolyte membranes for fuel cell. Polym Degrad Stab 2007;92:1289–96.
121. Choi P, Jalani NH, Datta R. Thermodynamics and proton transport in Nafion. I. Membrane swelling, sorption, and ion-exchange equilibrium. J Electrochem Soc 2005;152:E123–30.
122. Doyle M, Wang L, Yang Z, Choi SK. Polymer electrolytes based on ionomeric copolymers of ethylene with fluorosulfonate functionalized monomers. J Electrochem Soc 2003;150:D185–93.
123. Acara O, Sena U, Bozkurtb A, Ataa A. Proton conducting membranes based on Poly(2,5-benzimidazole) (ABPBI)–Poly(vinylphosphonic acid) blends for fuel cells. Int. J. of Hydrogen Energy. 34 (2009) 2724 – 2730
124. Li Q, Jensen J, Savinell R.F., Bjerrum N.J. High temperature proton exchange membranes based on polybenzimidazoles for fuel cells. Progress in Polymer Science. 34 (2009) 449–477.
125. Kawahara M, Morita J, Rikukawa M, Sanui K, Ogata N. Synthesis and proton conductivity of thermally stable polymer electrolyte: poly(benzimidazole) complexes with strong acid molecules. Electrochim Acta 2000;45:1395–8.
126. Xing BZ, Savadogo O. The effect of acid doping on the conductivity of polybenzimidazole (PBI). J New Mater Electrochem Syst 1999;2:95–101.
127. Pu HT, Meyer WH, Wegner G. Proton transport in polybenzimidazole blended with H3PO4 or H2SO4. J Polym Sci 2002;40B:663–9.

128. He RH, Li QF, Xiao G, Bjerrum NJ. Proton conductivity of phosphoric acid doped polybenzimidazole and its composites with inorganic proton conductors. J Membr Sci 2003;226:169–84.
129. Ma YL, Wainright JS, Litt MH, Savinell RF. Conductivity of PBI membranes for high-temperature polymer electrolyte fuel cells. J Electrochem Soc 2004;151:A8–16.
130. Akita H, Ichikawa M, Nosaki K, Oyanagi H, Iguchi M. Solid polymer electrolytes (Honda). US patent 6,124,060 (2000).
131. He RH, Li QF, Jensen JO, Bjerrum NJ. Doping phosphoric acid in polybenzimidazole membranes for high temperature proton exchange membrane fuel cells. J Polym Sci A: Polym Chem 2007;45:2989–97.
132. Taeyun Ko, Kihyun Kim, Min-Young Lim, Sang Yong Nam, Tae-Ho Kim, Sung-Kon Kim and Jong-Chan Lee. Sulfonated poly(arylene ether sulfone) composite membranes having poly(2,5-benzimidazole)-grafted graphene oxide for fuel cell applications. J. Mater. Chem. A, 2015,3, 20595
133. Proton conducting membranes based on Poly(2,5-benzimidazole) (ABPBI)–Poly(vinylphosphonic acid) blends for fuel cells. Int. J. of Hydrogen Energy. 34 (2009) 2724 – 2730
134. Asensio J., Sanchez E., Romero P. Proton conducting membranes based on benzimidazole polymers for high-temperature PEM fuel cells. Chem. Soc. Rev., 2010, 39, 3210-3239.
135. Asensio J., Sanchez E., Romero P. Proton conducting membranes based on benzimidazole polymers for high-temperature PEM fuel cells. J. Polym. Sci., Part A: Polym. Chem., 2002, 40, 3703-3710.
136. J. Weber, K. D. Kreuer, J. Maier and A. Thomas, Adv. Mater., 2008, 20, 2595–2598.
137. Tsung-Hsien Tang, Po-Hao Su , Yu-Chen Liu , T. Leon Yu.Polybenzimidazole and benzyl-methyl-phosphoric acid grafted polybenzimidazole blend crosslinked membrane for proton exchange membrane fuel cells. Int. J. Hydrogen Chem. 39 (2014) 11145 – 11156.
138. LaConti AB, Hamdan M, McDonald RC. Mechanisms of membrane degradation. In: Vielstichm W, Lamm A, Gasteiger HA, editors. Handbook of fuel cells, vol. 3. John Wiley & Sons Ltd.; 2003. p.647–62.
139.
140. Gaudiana RA, Conley RT. Weak-link versus active carbon degradation routes in oxidation of aromatic heterocyclic systems. J PolymSci 1969;7B:793–8.
141. Li Q, Pan C, Jensen JO, Noyé P, Bjerrum NJ. Cross-linked polybenzimidazole membranes for fuel cells. Mater Chem 2007;19:350–2.

142. Li Q, Jensen JO, Pan C, Bandur V, Nilsson M, Schönberger F, et al. Partially fluorinated arylene polyethers and their ternary blends with PBI and H3PO4, part II. Characterizations and fuel cell tests of the ternary membrane. Fuel Cells 2008;8:188–99.
143. Wang Y., Wang S., Xiao M., Han D., Meng Y. Preparation of a novel layer-by-layer composite membrane for vanadium redox flow battery (VRB) applications. Int. J. Hydrogen Energy. 39 (2014) 16088-16095.
144. He RH, Li QF, Bach A, Jensen JO, Bjerrum NJ. Physicochemical properties of phosphoric acid doped polybenzimidazole membranes for fuel cells. J Membr Sci 2006;277:38–45.
145. Xiao LX, Zhang HF, Scanlon E, Ramanathan L S, Choe EW, Rogers D, et al. High-temperature polybenzimidazole fuel cell membranes via a sol–gel process. Chem Mater 2005;17:5328–33.
146. Xiao L, Zhang H, Jana T, Scanlon E, Chen R, Choe EW, et al. Synthesis and characterization of pyridine-based polybenzimidazoles for high temperature polymer electrolyte membrane fuel cell applications. Fuel Cells 2005;5:287–95.
147. Li Q, Jensen JO, Pan C, Bandur V, Nilsson M, Schönberger F, et al. Partially fluorinated arylene polyethers and their ternary blends with PBI and H3PO4, part II. Characterizations and fuel cell tests of the ternary membrane. Fuel Cells 2008;8:188–99.
148. Li Q, Pan C, Jensen JO, Noyé P, Bjerrum NJ. Cross-linked polybenzimidazole membranes for fuel cells. Mater Chem 2007;19:350–2.
149. Fan Zhang, Xujin Bao, Qingting Liu, Mengyao Huang. High Temperature Polymer Electrolyte Membranes Based on Poly(2,5-benzimidazole) (ABPBI) and POSS Incorporated Ionic Liquid. Journal of Materials and Chemical Engineering . 2014, Vol. 2 Iss. 4, PP. 86-93.
150. Kreuer KD. On the complexity of proton conduction phenomena. Solid State Ionics 2000;136–137:149–60.
151. Kreuer KD. Proton conductivity: materials and applications. Chem Mater 1996;8:610–41.
152. Agmon N. The Grotthuss mechanism. Chem Phys Lett 1995;244:456–62.
153. Bose S, Kuila T, Nguyen T, Kim N.H., Lau K, Lee J. Polymer membranes for high temperature proton exchange membrane fuel cell: Recent advances and challenges. Progress in Polymer Science 36 (2011) 813–843
154. Tuckerman ME, Marx D, Parrinello M. The nature and transport mechanism of hydrated hydroxide ions in aqueous solution. Nature 2002;417:925–9.
155. Zhang J., Zhang H., Wu J., Zhang J. PEM Fuel Cell Testing and Diagnosis.

156. Ortiz-Palacios, J.; Cardoso, J.; Manero, O. Production of macroporous resins for heavy-metal removal. I. Nonfunctionalized polymers. J. Appl. Polym. Sci. 2008, 107, 2203–2210.

157. Courtois, J.; Szumski, M.; Georgsson, F.; Irgum, K. Assessing the macroporous structure of monolithic columns by transmission electron microscopy. Anal. Chem. 2006, 79, 335–344.

158. Drake, R.; Dunn, R.; Sherrington, D.C.; Thomson, S.J. Optimisation of polystyrene resin-supported pt catalysts in room temperature, solvent-less, oct-l-ene hydrosilylation using methyldichlorosilane. Comb. Chem. High Throughput Scr. 2002, 5, 201–209.

159. Deleuzel, H.; Schultze, X.; Sherrington, D.C. Porosity analysis of some poly(styrene/ divinylbenzene) beads by nitrogen sorption and mercury intrusion porosimetry. Polym. Bull. 2000, 44, 179–189.

160. Tang, X.; Wang, X.; Yan, J. Water-swellable hydrophobic porous copolymer resins based on divinylbenzene and acrylonitrile. II. Pore structure and adsorption behavior. J. Appl. Polym. Sci. 2004, 94, 2050–2056.

161. Blondeau, D.; Bigan, M.; Ferreira, A. Experimental-design study of the influence of the polymerization conditions on the characteristics of copolymers used for liquid chromatography. Chromatographia 2000, 51, 713–721.

162. Verweij, P.D.; Sherrington, D.C. High-surface-area resins derived from 2,3-epoxypropyl methacrylate cross-linked with trimethylolpropane trimethacrylate. J. Mater. Chem. 1991, 1, 371–374.

163. Hao, D.-X.; Gong, F.-L.; Wei, W.; Hu, G.-H.; Ma, G.-H.; Su, Z.-G. Porogen effects in synthesis of uniform micrometer-sized poly(divinylbenzene) microspheres with high surface areas. J. Colloid Interface Sci. 2008, 323, 52–59.

164. Zhou, Z.H.; Ruan, J.M.; Zou, J.P.; Zhou, Z.C. Synthesis of poly-L-Lactide for scaffold materials by melt-Solid polycondensation. Polym.-Plast. Technol. Eng. 2007, 46, 1195–1199.

Chapter - III

Motivation and Plan of Present Work

1. AIMS AND OBJECTIVES OF PRESENT WORK

2. PLAN OF WORK

2.1. Materials Used

2.2. Experimental Method

2.2.1. Preparation of ABPBI Polymer

2.2.2. Membrane Casting

2.3. Characterisation Studies

2.3.1. Structural and morphological studies

2.3.2. Thermal Stability

2.3.3. Proton Conductivity

1. AIMS AND OBJECTIVES OF PRESENT WORK

Although extensive work has been reported for the preparation of porous PBI membranes [1-7], relatively less work has been reported for the preparation of porous ABPBI[8-9]. The incorporation of pores into the ABPBI matrix is expected to raise the acid and water uptake capacities of the membranes. This in turn, is expected to increase proton transfer across the membrane and enhance fuel cell performances. However, a concurrent loss in mechanical and thermo-oxidative stabilities as well as increased fuel crossover is feared.

The use of sodium chloride for preparation of porous polymers by salt leaching process has been reported for other applications[10-11]. However, the preparation of porous ABPBI membranes using sodium chloride has not been reported in literature to the best of our knowledge.

Thus, the objectives of the present work are :

- To synthesize of poly(2,5-benzimidazole) (ABPBI) polymer by a polycondensation reaction of the 3,4-diaminobenzoic acid monomer.
- To cast ABPBI membrane via solvent evaporation method.
- To cast porous ABPBI (pABPBI) membrane via salt leaching/solvent evaporation method.
- To conduct structural and morphological characterisations of the ABPBI membrane and pABPBI membrane.
- To examine presence and nature of pores in the pABPBI membrane.
- To measure the water and acid uptakes of ABPBI and pABPBI membranes.
- To study the thermal stabilities of pABPBI and ABPBI membranes using Thermogravimetric Analysis (TGA).
- To study the proton conductivity properties of ABPBI and pABPBI membranes using EIS Technique.

2. PLAN OF WORK

2.1. Materials Used:

All chemical agents and solvents listed were used as received:

a. 3,4-Diaminobenzoic acid (DABA, 94%, Alfa Aesar),
b. Polyphosphoric Acid (PPA, calculated as P2O5 about 83%, Spectrochem),
c. Methansulphonic Acid (MSA) (Pure, MERCK),
d. Sodium Chloride (Hi-Pure),
e. ortho-Phosphoric acid (88% GR, MERCK),

2.2. Methods of Synthesis:

2.2.1. Synthesis of ABPBI polymer

ABPBI was prepared by the polycondensation of the 3,4-diaminobenzoic acid (DABA) monomers in polyphosphoric acid (PPA), as reported earlier. [12] In a 3-necked flask placed in an oil bath, 3.04 gm of DABA (20 milimoles) was stirred into 70gms of PPA at 150°C using a mechanical stirrer. After stirring for 30 min, temperature was raised to 200°C and the mixture was further stirred for 4 hours. The solution turned highly viscous and could not be poured out of the reaction vessel. Cold distilled water was poured into the flask, coagulating the mixture and arresting further polymerisation. Resulting polymer was washed with water and then 10% Ammonium hydroxide solution for a day to neutralise all residual phosphopric acid. Further washing with distilled water and acetone followed, before cutting and drying at 110°C for 24 hours to obtain the ABPBI granules.

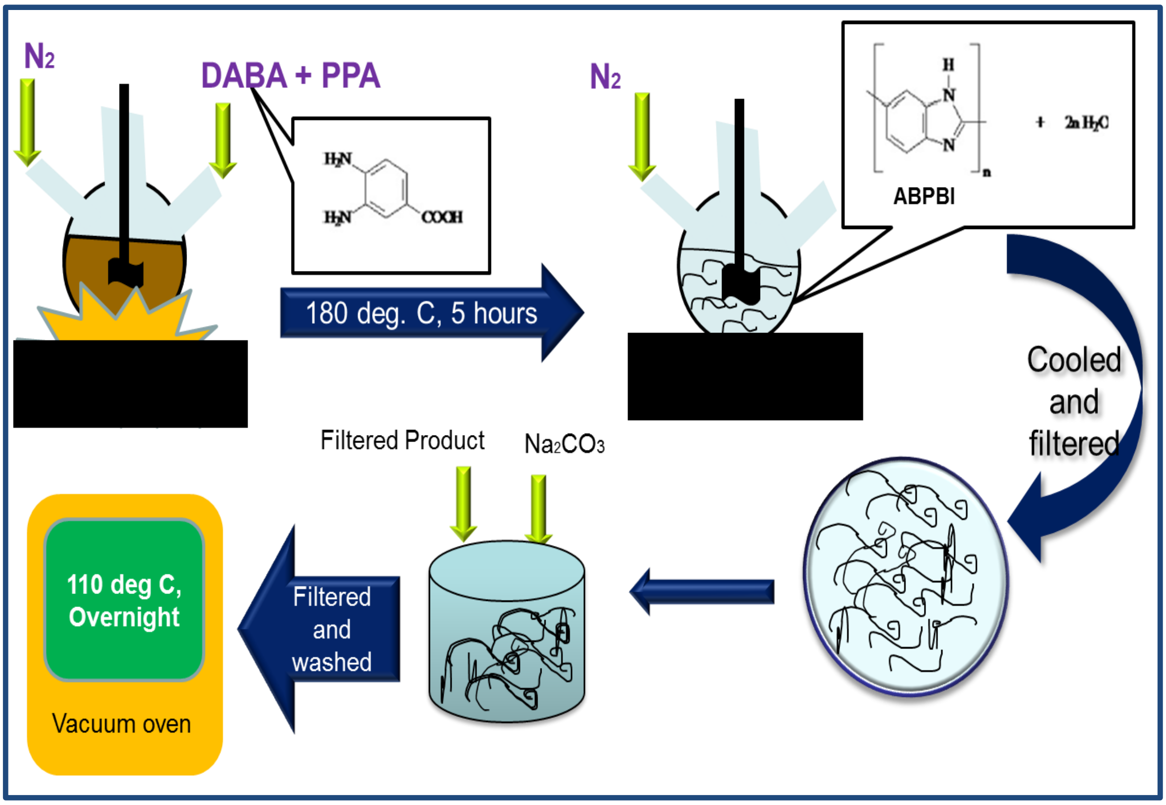

Fig 3.1. Schematic for Polymer Preparation.

Fig. 3.2. Polymerisation Setup with three-necked flask containing polymerisation mixture, being heated in an oil bath and stirred using mechanical stirrer.

Fig 3.3.: (left) Polymerisation arrest by pouring polymer mixture into cold water. (right top and middle) Thread like ABPBI polymer obtained. (right bottom) Cut and dried ABPBI polymer granules.

2.2.2. Membrane Casting:

Membranes were cast by solvent evaporation method. [12] The ABPBI was dissolved in Methanesulphonic Acid at ~150–180˚C for 3 hours to form a 4% solution. The viscous solution was then poured onto a flat bottomed Petridis and the solvent was evaporated at ~200˚C under a ventilated hood until volatility ceased. The membranes were then cooled down to 100˚C and hot water was poured into the Petridis to peel them off. All residual MSA was then extracted by repeatedly washing the membranes in boiling distilled water for several hours.

The porous ABPBI membrane (pABPBI) was prepared by salt leaching. Sodium Chloride was added to a prefixed amount of MSA required to make 4% ABPBI solution with 20%wt/wt polymer/salt concentration. The rest of the procedure was the same as for preparing the dense membranes. Washing the membranes were hot boiling water and then soaking them for several days in distilled water removed the salt embedded in the matrix.

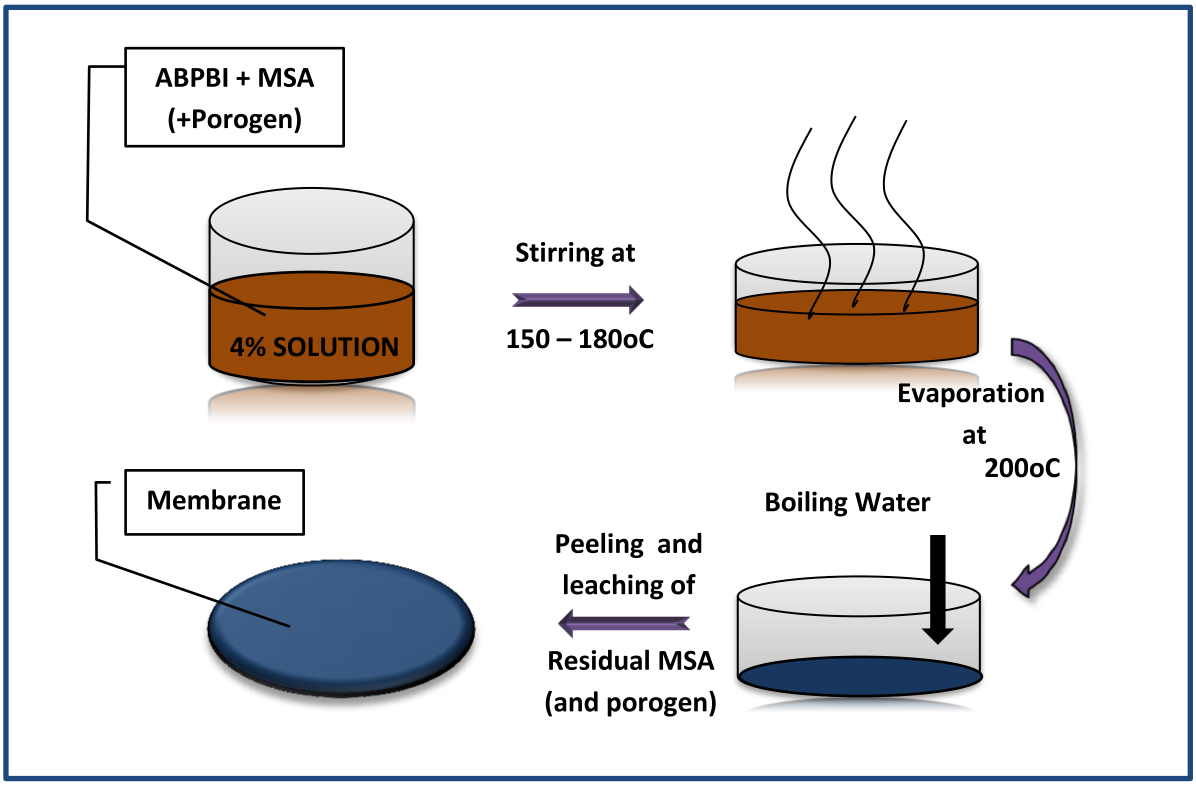

Fig. 3.4 Schematic for membrane casting procedure.

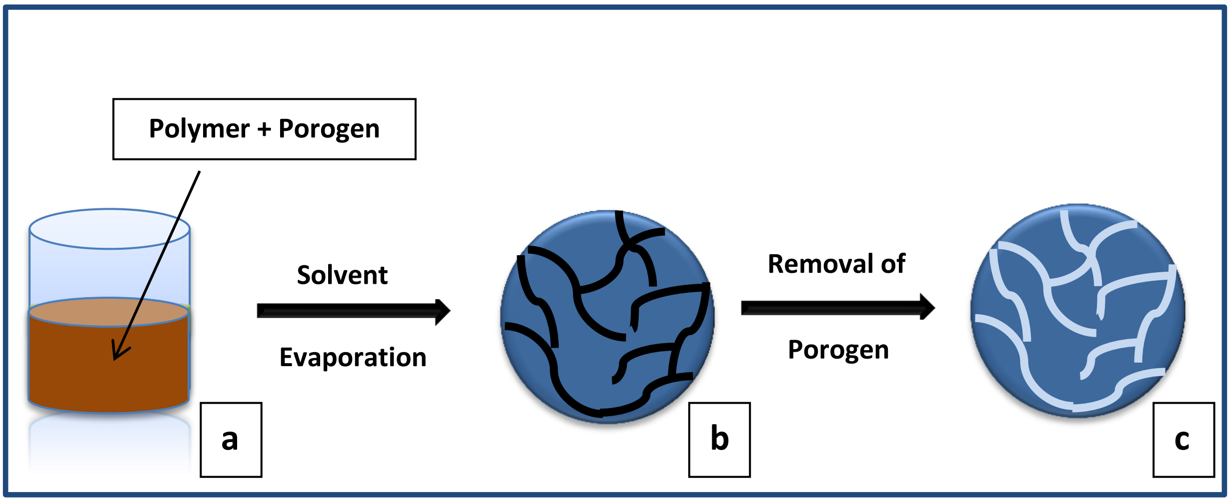

Fig. 3.5. Schematic representation of porous membrane preparation: (a) Reaction mixture containing polymer and porogens; (b) Polymer membrane containing porogen; (c) Porous Polymer membrane obtained after salt leaching.

2.3. Characterisation Studies

2.3.1. Structural and morphological studies:

- FT-IR spectra of the membranes were obtained on an IR-Prestige FTIR spectroscope (Shimadzu, Japan) over the frequency range from 3500 to 500 cm^{-1}.

- Scanning Electron Microscopy images were obtained to inspect the surface morphology of the membranes using a JSM-6700F (JEOL, Japan) for the purpose.

- An estimate of the surface porosity of the membranes was made by the use of NIS – Elements D software on SEM images. An area fraction estimate was made manually to get an estimate of porous surface to matrix.

2.3.2. Water and Phosphoric Acid Uptake

- Dry membrane samples were kept immersed in distilled water water for upto five days, and then rubbed with a tissue paper before being weighed quickly. The water uptake was calculated as [13]:

$$\text{Water Uptake \%} = \{(W_{wet} - W_{dry}) / W_{dry}\} * 100\%$$

where, W_{wet} and W_{dry} are the weights of the dry and wet membranes respectively.

- Acid uptake percentages were calculated in a similar manner by doping the dry membranes in ~ 60% H_3PO_4 for upto five days. The samples were then rubbed with tissue paper to remove surface adherent acid, dried in an oven to remove absorbed water and then weighed. The percentage acid uptakes were calculated as[14] :

$$\text{Percentage acid uptake} = \frac{(Wd - Wud)}{Wud} * 100\%$$

Where, W_d and W_{ud} are the dry weights of the doped and updoped membranes respectively.

2.3.3. Thermal Stability:

Thermogravimetric Analysis (TGA) of the acid doped membrane samples were carried out by heating the samples from 30°C to 750°C at the rate of 20°C/min. Each sample was dried in an oven and kept at room temperature for seven days before carrying out the tests.

2.3.4. Proton Conductivity:

The proton conductivity tests of the doped membranes were conducted using a two probe cell with circular (1cm diameter) silver electrodes and associated Metrohm AUTOLAB PGSTAT302N in the frequency range of 10^2–10^6 Hz with an amplitude of 0.01 V at different temperatures. The membranes were cut into circles of 1cm diameter and the values of the conductivities were calculated according to the following equation[15]:

$$\boldsymbol{\sigma = \frac{l}{A} \text{ x } \frac{1}{R}}$$

where,

σ is the proton conductivity in the direction of thickness of the membranes,

A is cross-sectional area of the membrane (with 1cm dia) = $\pi*(0.5)^2$ cm^2,

l is the thickness of the membrane = 0.005 cm

R is ohmic resistance as obtained from the equivalent circuit fit given by EIS studies.

REFERENCE

1. L. Zeng, T. S. Zhao, L. An, G. Zhao and X. H. Yan. A high-performance sandwiched-porous polybenzimidazole membrane with enhanced alkaline retention for anion exchange membrane fuel cells. Energy Environ. Sci., 2015, 8, 2768.
2. Li-Cheng Jheng, Steve Lien-Chung Hsu, Tzung-Yu Tsai and Wesley Jen-Yang Changa. A novel asymmetric polybenzimidazole membrane for high temperature proton exchange membrane fuel cells. J. Mater. Chem. A, 2014,2, 4225.
3. Hadis Zarrin, Gaopeng Jian, Grace Y.-Y. Lam, Michael Fowler, Zhongwei Chen. High performance porous polybenzimidazole membrane for alkaline fuel cells. Int. J. Hydrogen Energy. x x x (2014) 1-11.
4. Cheng-Hsun Shen, Li-cheng Jheng, Steve Lien-chung Hsu and Jacob Tse-Wei Wang. Phosphoric acid-doped cross-linked porous polybenzimidazole membranes for proton exchange membrane fuel cells. J. Mater. Chem., 2011, 21, 15660.
5. David Mecerreyes, Hans Grande, Oscar Miguel, Estibalitz Ochoteco, Rebeca Marcilla, and Igor Cantero. Porous Polybenzimidazole Membranes Doped with Phosphoric Acid: Highly Proton-Conducting Solid Electrolytes. J. Chem. Mater. 2004, 16, 604-607.
6. Jin Li, Xiaojin Li, Shuchun Yu, Jinkai Hao, Wangting Lu, Zhigang Shao, Baolian Yi. Porous polybenzimidazole membranes doped with phosphoric acid: Preparation and application in high-temperature proton-exchange-membrane fuel cells. Energy Conversion and Management 85 (2014) 323–327.
7. Dongju Chen, Shanshan Yu, Xue Liu, Xianfeng Li. Porous polybenzimidazole membranes with excellent chemical stability and ion conductivity for direct borohydride fuel cells. Journal of Power Sources 282 (2015) 323-327.
8. Haitao Zheng, Leslie Petrik, Mkhulu Mathe. Preparation and characterisation of porous poly(2,5benzimidazole) (ABPBI) membranes using surfactants as templates for polymer electrolyte membrane fuel cells. Int. J. Hydrogen Energy x x x (2010) 1–6.
9. US 2013/0053467 A1. Feb. 28, 2013. Ulhas Kharul, Harshada Lohokare. Porous Abpbi [Poly (2,5-Benzimidazole)] Membrane And Process Of Preparing The Same.

10. An-Chong Chao, Shu-Huei Yu, Guo-Syong Chuang. Using NaCl particles as porogen to prepare a highly adsorbent chitosan membranes. Journal of Membrane Science 280 (2006) 163–174.
11. Zhihua Zhou, Xiaoping Liu, And Qingquan Liu. A Comparative Study of Preparation of Porous Poly-L-lactide Scaffolds Using NaHCO3 and NaCl as Porogen Materials. Journal of Macromolecular Science, Part B, 47:4, 667-674.
12. Juan Antonio Asensio, Salvador Borro´s, and Pedro Go´mez-Romero. Polymer Electrolyte Fuel Cells Based on Phosphoric Acid-Impregnated Poly„2,5-benzimidazole Membranes. Journal of The Electrochemical Society, 151 (2) A304-A310 (2004).
13. Taeyun Ko, Kihyun Kim, Min-Young Lim, Sang Yong Nam, Tae-Ho Kim, Sung-Kon Kima and Jong-Chan Lee. Sulfonated poly(arylene ether sulfone) composite membranes having poly(2,5-benzimidazole)- grafted graphene oxide for fuel cell applications. J. Mater. Chem. A, 2015,3, 20595.
14. Mao Linlin,Ananta Kumar Mishra, Nam Hoon Kim, Joong Hee Lee. Poly(2,5-benzimidazole)–silica nanocomposite membranes for high temperature proton exchange membrane fuel cell. Journal of Membrane Science 411–412 (2012) 91– 98.
15. Xujin Bao, Fan Zhang, Qingting Liu. Sulfonated poly(2,5-benzimidazole) (ABPBI)/ MMT/ ionic liquids composite membranes for high temperature PEM applications. Int. J. Hydrogen Energy. 40 (2015) 16767-16774.

Chapter - IV

Results and Discussion

1. **MEMBRANE APPEARANCE**

2. **FT-IR SPECTROSCOPY**

3. **SCANNING ELECTRON MICROGRAPHS**

4. **WATER AND ACID UPTAKES**

5. **THERMAL STABILITY ANALYSIS**

6. **PROTON CONDUCTIVITY STUDIES**

1. MEMBRANE APPEARANCE:

Wainright et al have[1] reported the preparation of ABPBI polymer with inherent viscosities as high as 7.33 dl/g by recrystalisation of the monomer. However, Asensio et al. [2] have reported that polymers with inherent viscosities of 2.2 - 2.4 dl/gm are enough to cast membranes of suitable strengths. Polymer prepared in the case of present study had a high enough degree of polymerisation to give membranes with adequate thermo-mechanical strengths that were substantially stable even when doped in acid.

Fig. 4.1 (a) top (left) and bottom (right) surfaces of ABPBI membrane

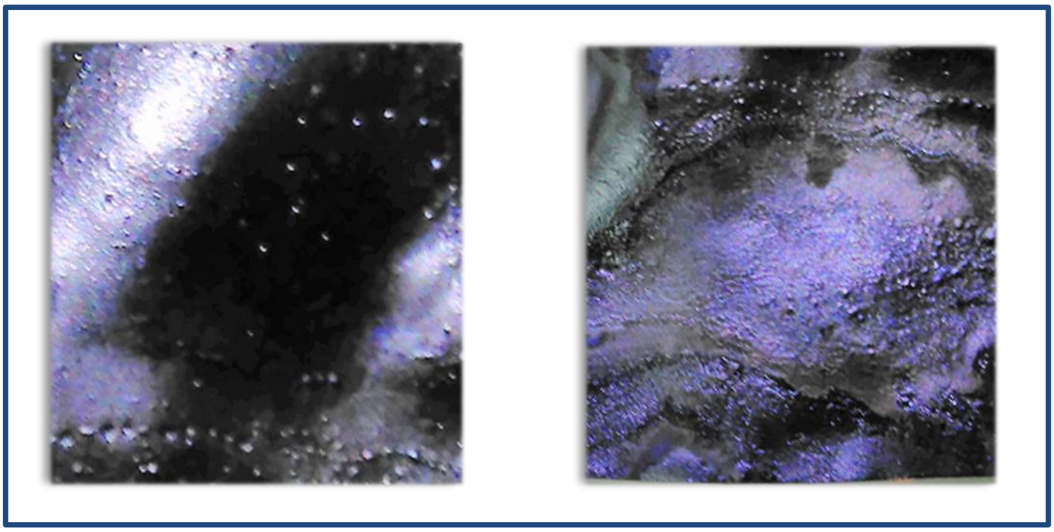

Fig. 4.1(b) top (left) and bottom (right) surfaces of pABPBI membrane

The pristine ABPBI (Fig. 4.1.) appears smooth on both surfaces without pinholes, suggesting homogenous membrane formation. The presence of occasional pinholes and striations are noticed in the pABPBI membrane (Fig. 4.2) with the introduction of the salt, suggesting difficulty in sol-gel transition. [3]

2. FT – IR SPECTROSCOPY:

Fig. 4.2. shows the FTIR spectra of the ABPBI and porous ABPBI polymer. The band assignements have been done as per Table 3.1. [4-6] The spectra of the porous membranes are almost identical to that of the pristine membrane with slight shifts due to the changes in chemical environment.

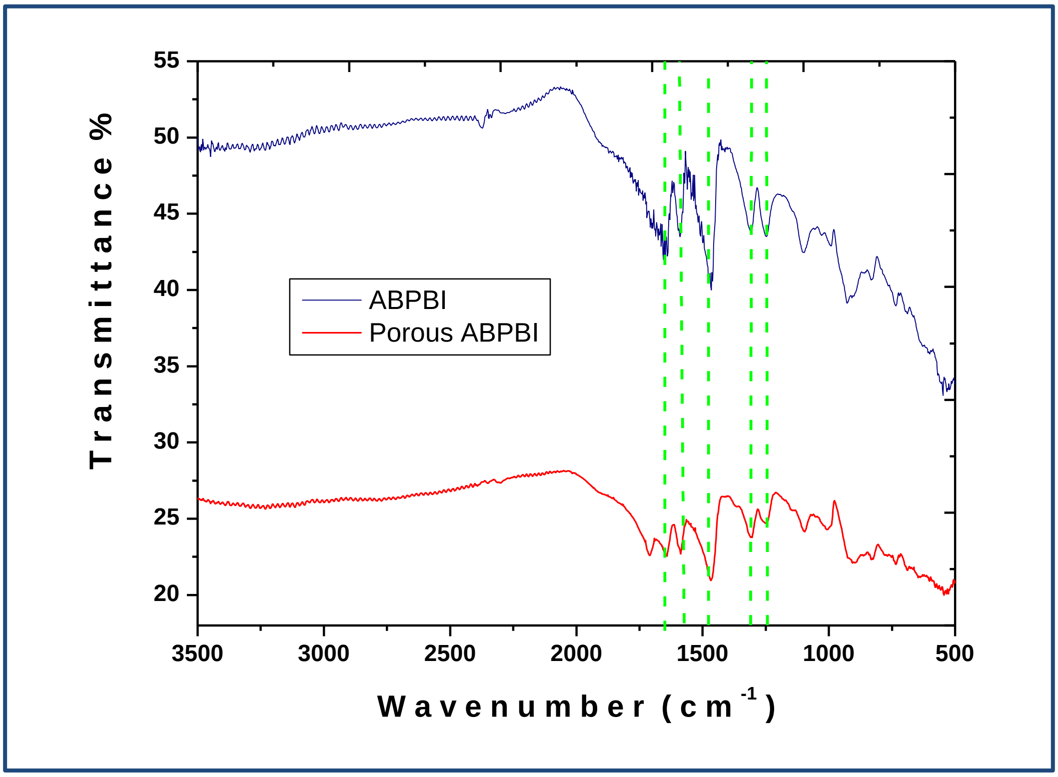

Fig. 4.2. FT-IR spectra of ABPBI and porous ABPBI

The broad bands in the region of 3500-2000cm^{-1} are indicative of N-H stretchings ("free" and associated) of the imidazole ring. The peaks have broadened in the presence of moisture. The C=C and C=N stretchings are attributable to the relatively sharp peaks centred around 1650cm^{-1} and 1550cm^{-1} for both membranes. The imidazole ring breathing mode and the inplane deformation of the benzimidazole ring correspond to the peaks centred around 1309 and 1247 respectively . The residual MSA is seen to absorb in the range of 1090 - 1100cm^{-1}.

3. SCANNING ELECTRON MICROGRAPHS:

The SEM micrographs shown in Fig. 4.3. and 4.4. reveal the evidently porous structures of the modified membrane. The ABPBI membrane shows a smooth surface without pinhole defects. Spherical micro and mesopores are seen on the surface of the pABPBI membrane. There is presence of bigger macropores on the surface of the porous membranes, which may have resulted due to uneven drying during casting.

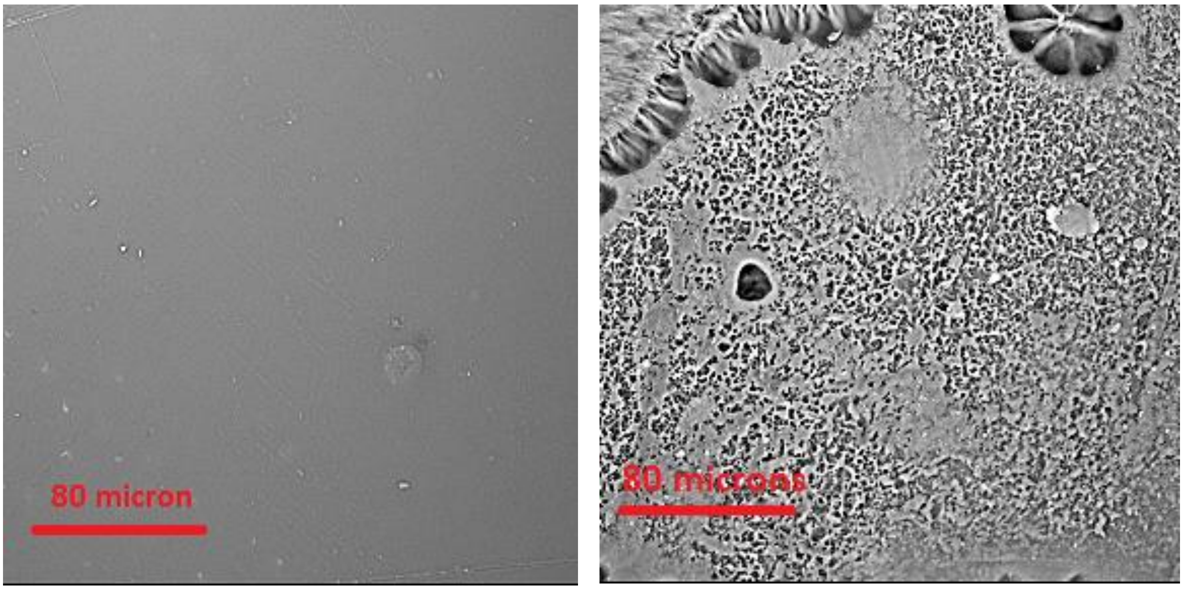

Fig. 4.3.: SEM Micrographs of ABPBI (left) and pABPBI (right) membranes

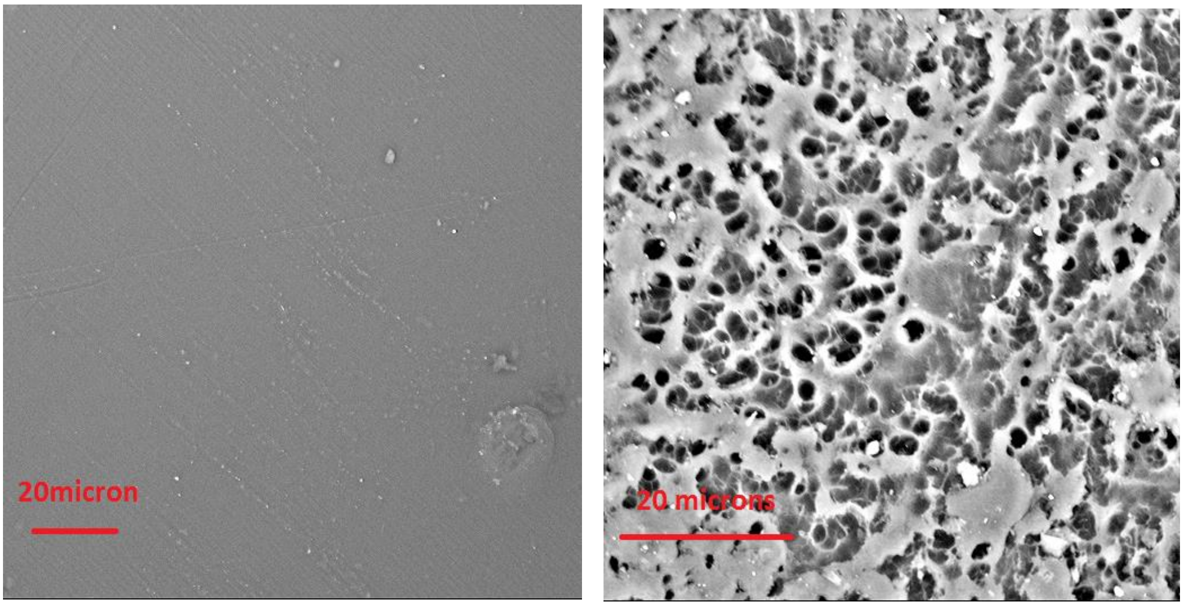

Fig. 4.4.: SEM micrographs of ABPBI (left) and pABPBI membranes (right) at higher magnification.

The cross-sectional SEM micrographs of the membranes are shown in Fig. 6.5.

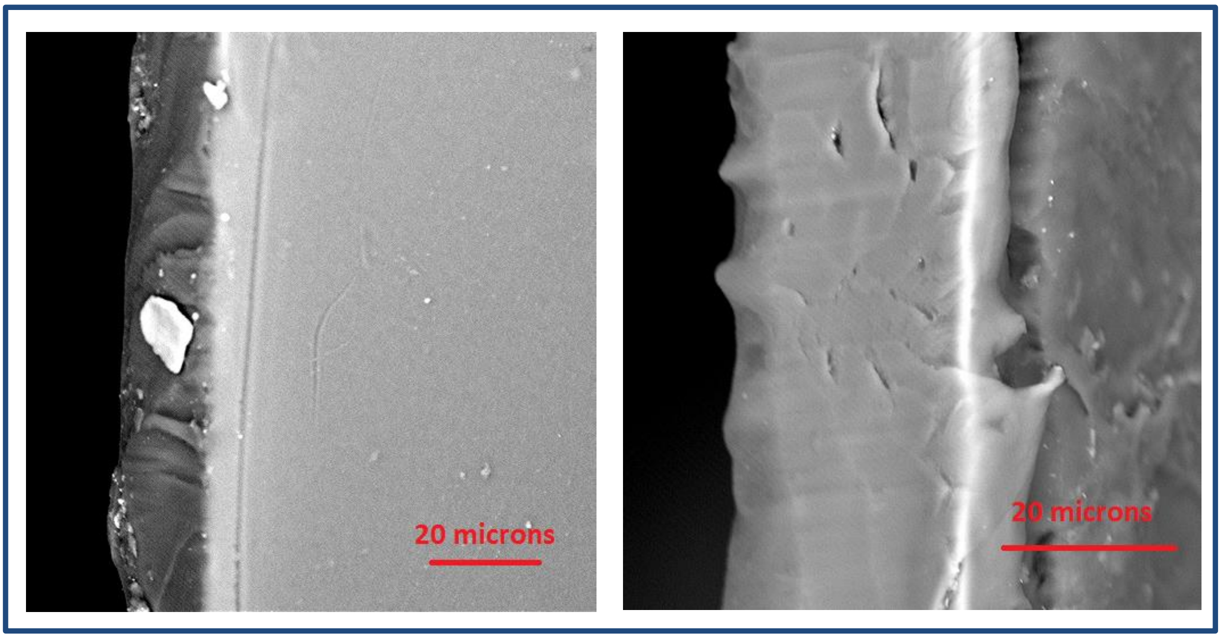

Fig. 4.5. Cross-sectional SEM images for ABPBI (left) and pABPBI (right) membranes

The ABPBI membrane shows signs of agglomerates but is dense otherwise. The porous membrane shows signs of occasional isolate reticulate holes embedded within the matrix with little interconnection within the matrix. The pore fraction area is manually calculated to be 22.22% compared to total area using NIS-Elements D software as shown in Fig . 4.6.

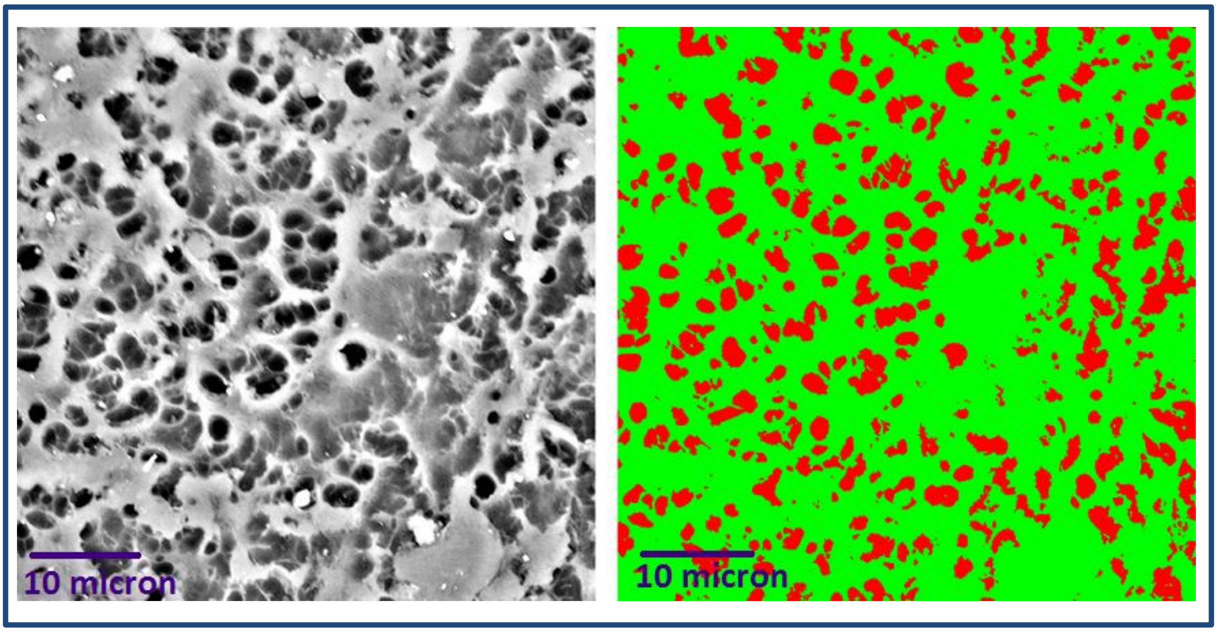

Fig 4.6. Estimation of porous area of pABPBI membrane

4. WATER AND PHOSPHORIC ACID UPTAKE:

Water uptake capacities of membranes is one of the factors affecting proton conductivity. Fig. 4.7. shows the water uptake percentages of the pristine and porous membrane.

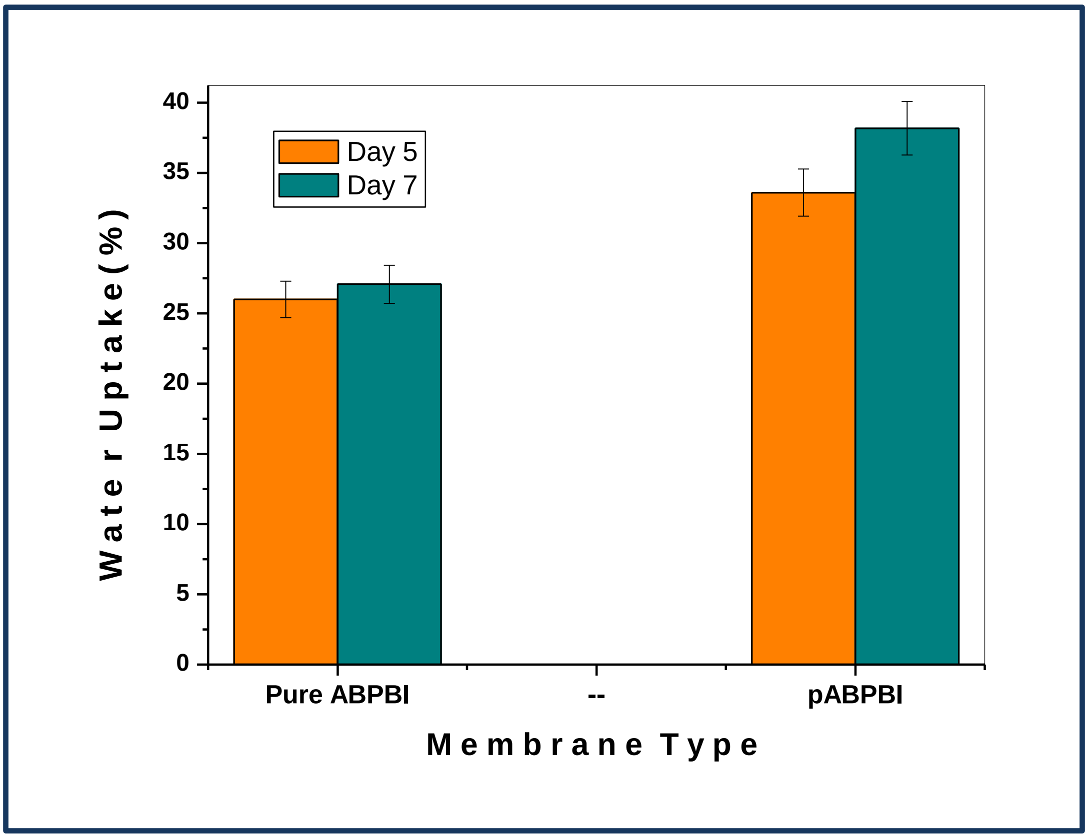

Fig. 4.7 . Water Uptake Percentages of Pure and pABPBI membranes

The porous membrane is seen to exhibit an improved water and acid uptake as compared to the plain membrane. For the pABPBI membrane, water uptake percentage increases to ~ 34% from an initial value of 26% for the pristine ABPBI. ABPBI is known to be hygroscopic by itself [2] and the increasing uptakes is attributable to the retention of moisture due to entrapment in the pores. There is no significant swelling or reduction in mechanical strengths due to moisture absorption.

The membranes when dopes in phosphoric acid undergo a plasticizing effect that swells and softens the membranes considerably. For this, an optimized doping level is required which does not degrade membrane material at the cost of enhacing proton conductivity. The ABPBI membranes exhibit a maimum doping level of ~200% as shown in fig 4.8. The doped porous membranes shows an increase from this maximum possible by entrapping liquid acid within the porous matrix.

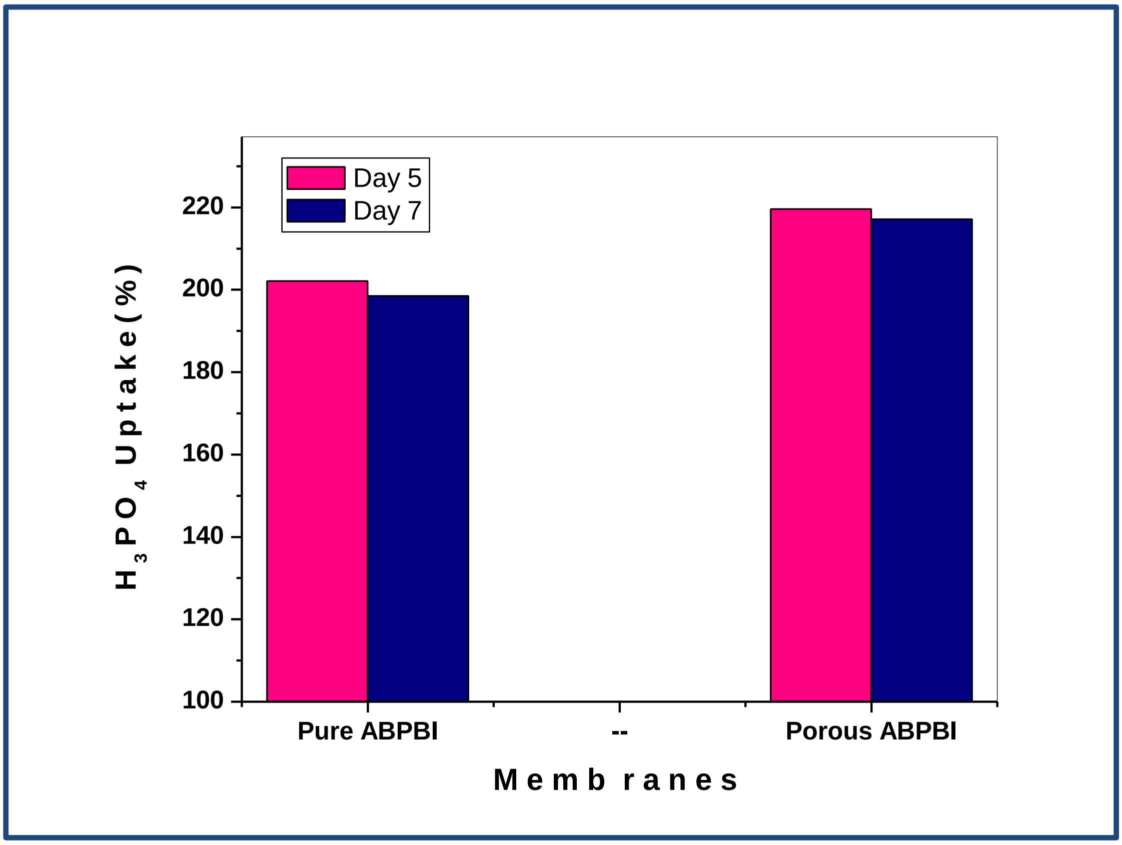

Fig. 4.8. Phosphoric Acid Uptake Percentage of ABPBI and pABPBI membranes

Complementary to the water uptake trend, the acid uptake percentage of the pABPBI membrane is about 219.6 % as compared to 202.075% for pristine ABPBI (about 1.08 times higher). This is the desired result, since porous ABPBI is expected to retain more acid within the pores. The decrease in mass on the 7th day may be attributable to a degradation of the membrane matrix in the acid.

5. THERMAL STABILITY ANALYSIS:

Polymeric membranes are expected to exhibit good thermal stabilities under the working temperatures of a fuel cell. It is well known that the poly(2,5-benzimidazole) has high thermal stabilities upto 600°C[1-3]. This is evident from the graph shown in Fig. 4.9. There are two mass loss zones present. The mass loss below 150°C is attributable to the loss of absorbed moisture. Evidently, due to its capillarity, the pABPBI membrane has retained a higher degree of moisture and shows a loss of 15% weight loss at 100°C as compared to a 10% weight loss for the ABPBI membrane. There is a gradual weight loss upto 600°C, whereafter the membranes begin to disintegrate. Overall, both membranes show acceptable thermal stabilities within the working temperature ranges of the HT-PEMFC.

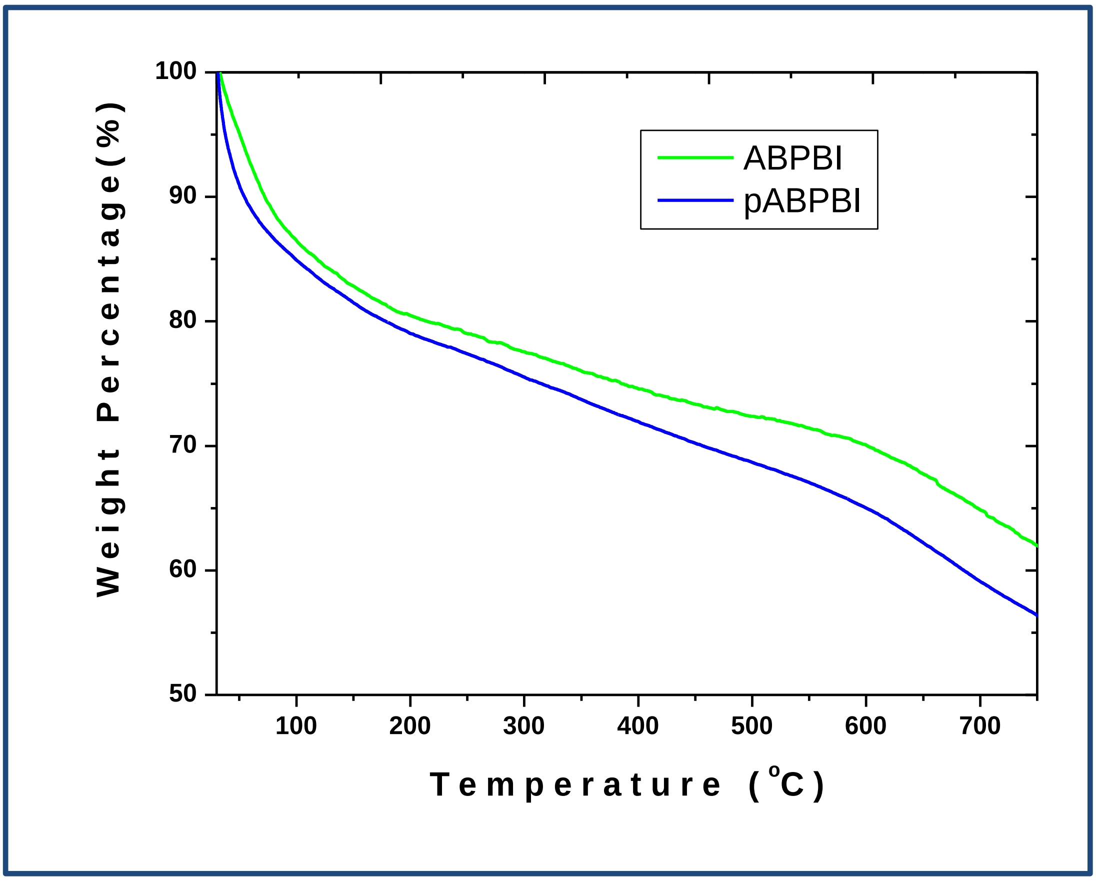

Fig. 4.9. Thermogravimetric analysis of ABPBI and pABPBI membranes.

The DSC curves of the pristine and porous membranes are shown in Fig. 4.10. [7] suggested that the existence of a single endothermic peak sis due to the release of moisture attached to the homogenous polymeric membrane.

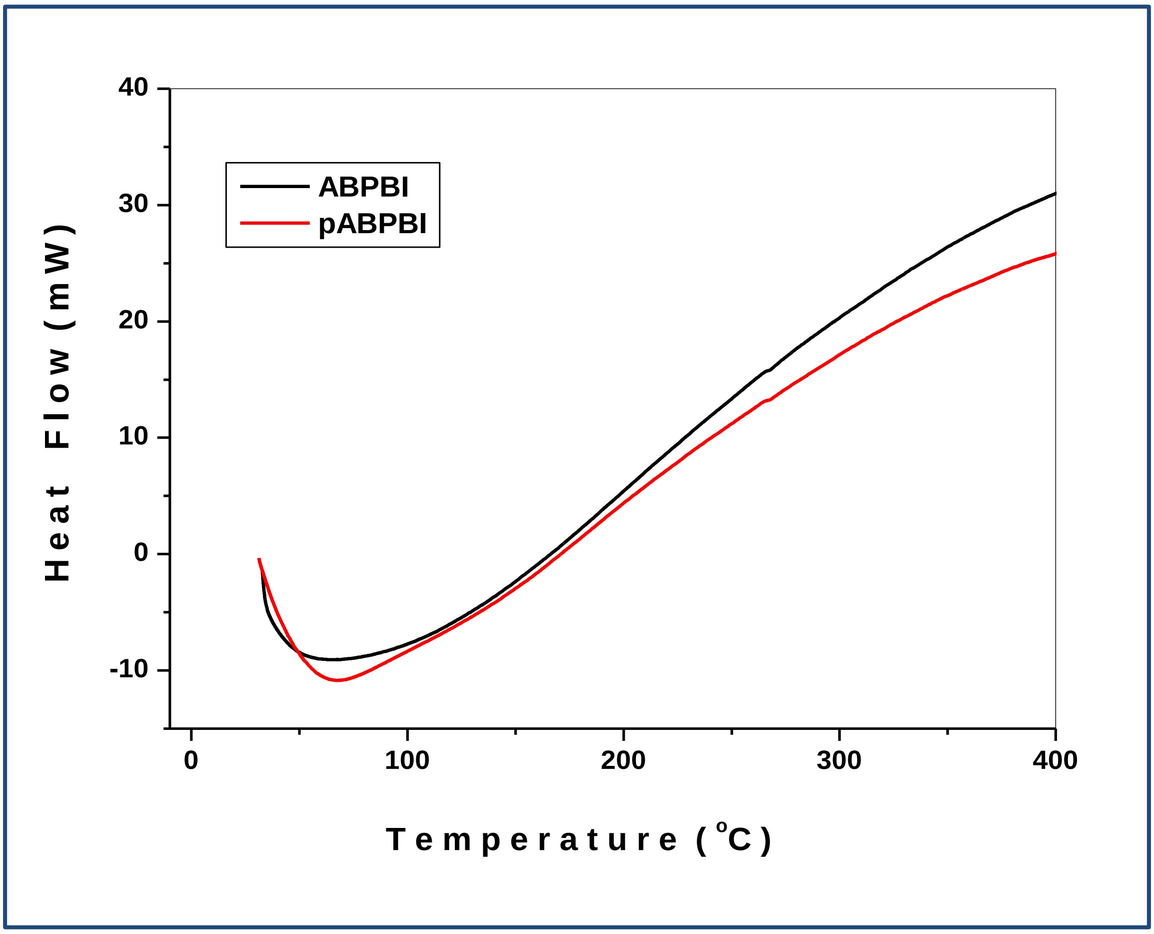

Fig. 4.10. Differential Scanning Calorimetry curves for ABPBI and pABPBI membranes.

6. PROTON CONDUCTIVITY

Poroton conductivity readings indicate an increase in proton conduction with increasing temperature for both membranes. However, the rise in conductivity values for the porous ABPBI membrane is much higher than that for the dense ABPBI membrane. This is the expected behaviour as the former reports a higher acid and water capacity than the latter, possibly due to the presence of pores which act as reservoirs, trapping the dopant.

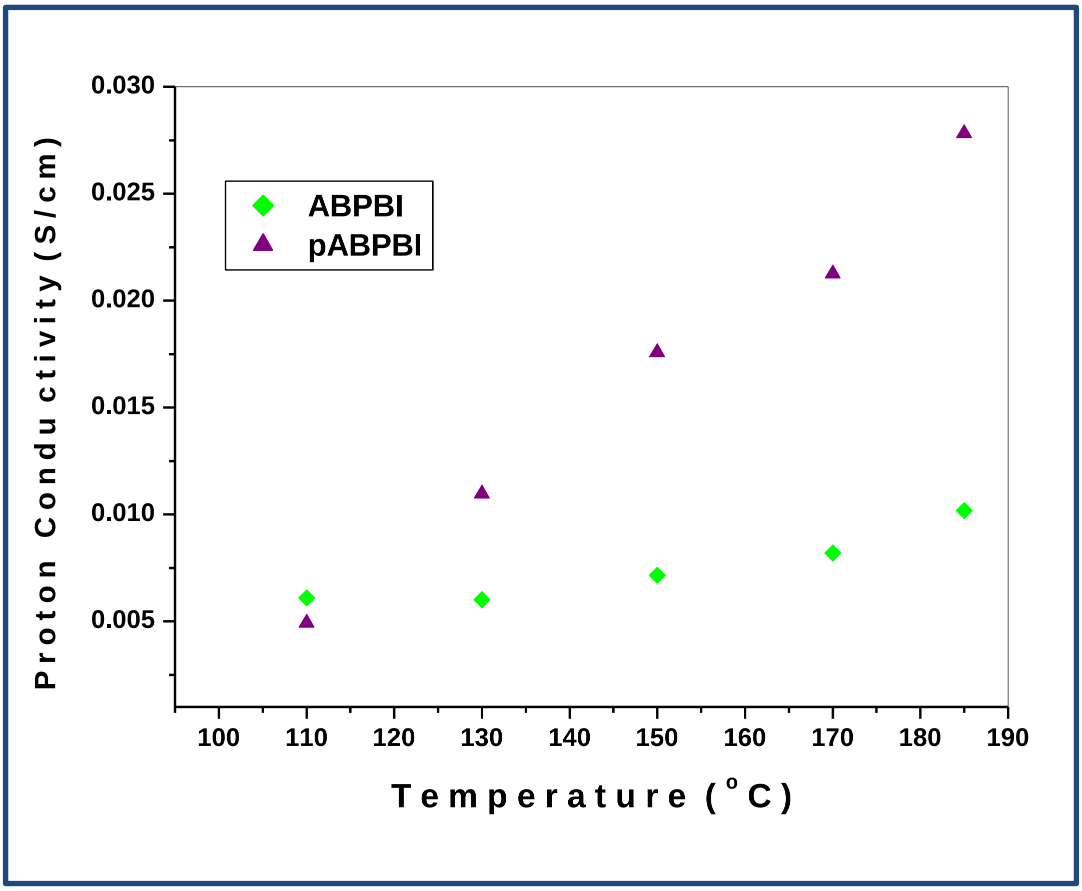

Fig 4.11. Proton conductivities of ABPBI and pABPBI membranes at different temperatures.

According to Ma et al.[8] the rate of proton transfer by free acid to free water is of the highest order amongst all other proton hopping pathways. Correspondingly, it may be suggested that the "acid wells" trapped within the porous matrix of the pABPBI are the reason for the steep rise in proton conductivity values as seen above. A maximum conductivity of 0.02783 S/cm was achieved for the pABPBI membrane as compared to 0.01019S/cm for ABPBI membrane at 185°C.

REFERENCE

1. Wainright J.S., Litt M.H., Savinell R.F. in Handbook of Fuel Cells, Funddamentsals, Technology, and Applications, Vol 3, (Eds. W. Vielstich, A. Lamm, H.A. Gasteiger), John and Wiley Sons, New York, 2003.
2. Asensio, J,A., Gomez-Romero P. Recent Developsments of Proton Conducting Poly(2,5-benzimidazole) (ABPBI) membranes for high temperature polymer electrolyte membrane fuel cells. Fuel Cells, 2005, No 3.
3. Palanichamy Krishnan *, Jin-Soo Park, Chang-Soo Kim. Performance of a poly(2,5-benzimidazole) membrane based high temperature PEM fuel cell in the presence of carbon monoxide. J*ournal of Power Sources 159 (2006) 817–823*
4. Musto P, Karasz FE, Macknight WJ. Hydrogen-bonding in polybenzimidazole polyimide systems—a Fourier-transform infrared investigation using low-molecular-weight monofunctional probes. Polymer 1989; 30:1012–21.
5. Asensio J, Borro´s S and Romeroa P. Polymer Electrolyte Fuel Cells Based on Phosphoric Acid-Impregnated Poly(2,5-benzimidazole) Membranes. J. Electrochem Soc., 151 (2) A304-A310 (2004)
6. Ko T, Kim K, Lim M, Nam S, Kim T, Kima S and Lee J. Sulfonated poly(arylene ether sulfone) composite membranes having poly(2,5- benzimidazole)-grafted graphene oxide for fuel cell applications. J. Mater. Chem. A, 2015,3, 20595.
7. Ji-Ye Kang, Soo-Mi Eo, In-Yup Jeon, Yeong Suk Choi, Loon-Seng Tan, Jong-Beom Baek. Multifunctional Poly(2,5-benzimidazole)/Carbon Nanotube Composite Films. JOURNAL OF POLYMER SCIENCE: PART A: POLYMER CHEMISTRY DOI 10.1002/POLA
8. Y. Ma. PhD Thesis, Case Western Reserve University, 2004.

Chapter – V : Conclusions

An attempt was made to synthesize porous ABPBI membrane for high temperature fuel cell application. The porous matrix was investigated using Scanning Electron microscopes. SEM images revealed membranes with spherical mesopores mainly on the surface. NIS-Elements D software was used to estimate the surface porosity. It was found that 22.22% of the membrane surface was porous area and the rest was solid matrix. FT-IR spectroscopic images revealed that there has been no structural change due to the introduction of the salt. That is, all the salt has been effectively leached out by water washing after membrane casting. Water and acid uptake studies revealed an increase of 1.3 and 1.08 times increase respectively in the porous membrane. The porous matrix expectedly "trapped" the moisture and phosphoric acid, and retained them due to high capillarity. This was further supported by the enhanced proton conduction exhibited by pABPBI membrane. A maximum proton conductivity of about 30mS/cm was achieved for the pABPBI membrane at 185^{o}C, more than twice the value obtained for ABPBI membrane under similar conditions. Beyond 190^{o}C, both membranes showed a decrease in conductivity, possibly due to the breakdown of phosphoric acid into pyrophosphoric acid. The thermal stabilities of both membranes were also tested. It was seen that pABPBI reported a higher loss of mass below 150^{o}C (due to higher amounts of absorbed water retained within the porous structure). Both membranes were highly stable upto 600^{o}C, after which the polymer backbone began to disintegrate.

It is concluded that a porous ABPBI membrane with a thermally stable matrix and enhanced proton conductivity properties was successfully prepared. Thus, this membrane can potentially be used in High-Temperature Polymer Electrolytic Membrane Fuel Cells.